

**Nanofluid containing Cu – H₂O treated through
Maxwell model with induced magnetic field in
peristaltic**



By

Shafee Ahmad

216-FBAS/MSMA/F-14

**Department of Mathematics and Statistics
Faculty of Basic and Applied Sciences
International Islamic University, Islamabad
Pakistan**

2016



Accession No TH-16775 ^{VC}



MS
532.05
SHN

1. Fluid dynamics - Mathematical
models

**Nanofluid containing Cu – H₂O treated through
Maxwell model with induced magnetic field in
peristaltic**



By

Shafee Ahmad

Supervised by

Dr. Rahmat Ellahi

**Department of Mathematics and Statistics
Faculty of Basic and Applied Sciences
International Islamic University, Islamabad
Pakistan
2016**

**Nanofluid containing Cu – H₂O treated through
Maxwell model with induced magnetic field in
peristaltic**

By

Shafee Ahmad

**A Thesis
Submitted in the Partial Fulfillment of the
Requirements for the Degree of
MASTER OF PHILOSOPHY IN MATHEMATICS**

Supervised by

Dr. Rahmat Ellahi

**Department of Mathematics and Statistics
Faculty of Basic and Applied Sciences
International Islamic University, Islamabad
Pakistan**

2016

Declaration

I hereby declare and affirm that this research work neither as whole nor as a part has been copied out from any source. It is further declare that I have developed this research work entirely on the basis of my personal efforts. If any part of this thesis is proven to be copied out or found to be a reproduction of some other, I shall stand by the consequences.

Moreover, no portion of the work presented in this thesis has been submitted in support of an application for other degree or qualification in this other university or institute of learning.

Signature:-----

Shafee Ahmad

M.Phil Scholar (Mathematics)

216-FBAS/MSMA/F-14

Certificate

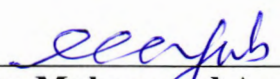
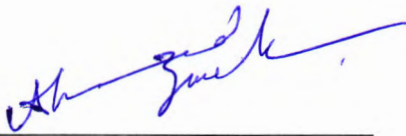
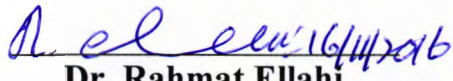
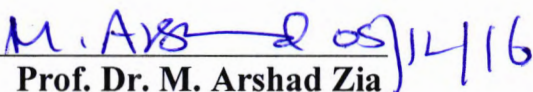
Nanofluid containing Cu – H₂O treated through Maxwell model with induced magnetic field in peristaltic

By

Shafee Ahmad

A DISSERTATION SUBMITTED IN THE PARTIAL FULFILLMENT OF THE REQUIREMENTS
FOR THE DEGREE OF THE MASTER OF SCIENCE IN MATHEMATICS

We accept this dissertation as conforming to the required standard.

1. 
Prof. Dr. Muhammad Ayub
(External Examiner)
2. 
Dr. Ahmed Zeeshan
(Internal Examiner)
3. 
Dr. Rahmat Ellahi
(Supervisor)
4. 
Prof. Dr. M. Arshad Zia
(Chairman)

**Department of Mathematics & Statistics
Faculty of Basic and Applied Sciences
International Islamic University, Islamabad
Pakistan
2016**

Dedication

This thesis is dedicated to Holy prophet

Hazrat Muhammad (P.B.U.H)

&

My family

Acknowledgements

Primarily and foremost, I am thankful to Almighty Allah, who is the only creator and master of us, who created us from a clot and taught us to write with the pen who provided me the strength and ability to learn and to achieve another milestone to a destination. Countless droods and slams upoun prophet Muhammad (SAW) who is forever a torch of gaudiness, a source of knowledge and blessings for entire creation. His teaching shows us a way to live with dignity, stand with honor and learn to be humble.

Foremost thanks go to my supervisor **Dr. Rahmat Ellahi**, his dynamic supervision, guidance in a right direction, constant moral encouragements and motivation of hard work made my task easy and I completed my dissertation well within time. His comprehensive knowledge and logical way of thinking have been of greater value for me. His understanding, encouraging and personal guidance have provided a good basis to understand the field of fluid mechanics. His ideas and concepts have remarkable influence on my research skills. I have learned a lot from him.

I am much indebted to my senior research fellow **Dr. Mohsan Raza** for his valuable advice in discussion, his precious time to guide and gave his comments. I truthfully acknowledge his for the ideas he enthusiastically shared with me to produce my best work. He really helped me out in every problem.

I am grateful to **Dr. Muhammad Arshad Zia** Chairman Department of Mathematics for providing assess to facilities that ensured successful completion of my work.

A warm thanks to **Mr. Muzanmal Hameed Tariq, Mr. Mohib-ur-Rahman, Mr. Ifraheem Waheed, Mr. Najib Ullah, Mr. Awais and Mr. Bilal Arain** Who offered me a lot of friendly help during my research work. Many thanks to **Dr. Ahmad Zeeshan, Dr. Nasir Ali, Dr. Mohsin Hassan and Dr. Ahmar**, for their valuable discussions that helped me to understand my research area in much a batter way.

Acknowledgements are incomplete without paying regards to my parents who've always given me perpetual love, care and cheers. Whose prayers have been a source of great inspiration for me and whose sustained hope in me led me to where I stand today. I have no words to thanks my Brothers **Mr. Sadiq Ahmad, Mr. Basir Ahmad** and **Sisters** who developed self-confidence and support me.

I am highly thankful to my relatives **Mr. Fazi-ur-Rahman and Mr. Farid-ullah** to their efforts, moral supports and love that I am as I am today.

Shafee Ahmad
17, Octobar, 2016

Preface

Nanofluid containing Cu – H₂O treated through Maxwell model with induced magnetic field in peristaltic is important in many processes. For the first time nanofluid was discussed by Choi [1] which refers to a conventional heat transfer fluid (Water, oil, ethylene glycol, etc.) which contains a dispersion of nano size particles. Majorly, the nanoparticles are considered to be used a tools to increase the thermal conductivities of the base fluids. The thermal conductivity of heating/cooling fluids plays a vital role in the development of energy efficient heat transfer equipment for electronics, transportation, energy supply, and production. The nanofluids actually contain tiny particles (~10 nm diameter) of a magnetic solid suspended in a liquid medium. For more detail see Refs. [2-10].

Peristalsis is a mechanism of fluid that flows through movement of contraction on the tubes/channels walls. First of all this concept was developed by Latham [11]. He described fluid motion in peristaltic pump. Further, he also explained the characteristic of pressure rise versus flow rate. Peristalsis is attracted thousands of researchers around the globe due to its wide applications in the industry and in the field of medicine, i.e., the heart–lung machine.

Moreover, the effects of magnetohydrodynamics (MHD) on peristaltic flow problems also have some applications in physiological fluids such as blood flow, blood pump machines, and theoretical studies on the operation of peristaltic MHD compressors. Due to these important practical applications researchers have put their attentions towards peristaltic flows see Refs. [12-17].

This thesis discusses the nanofluid containing Cu – H₂O treated through Maxwell model with induced magnetic field in peristaltic which are still not available in existing literature to the best of author knowledge.

The present thesis is arranged as follows:

Chapter one includes some relevant definitions and equations of the subsequent chapters.

Chapter two is a review work of [18].

Chapter three is the extension of chapter two in which the nanofluid containing Cu – H₂O treated through Maxwell model with induced magnetic field in peristaltic flow is investigated.

Contents

1 Preliminaries	3
1.1 Definition.....	3
1.1.1 Fluid.....	3
1.1.2 Peristalsis.....	3
1.1.3 Peristaltic transport.....	3
1.2 Types of fluids.....	3
1.2.1 Newtonian fluids.....	3
1.2.2 Non-Newtonian fluid.....	4
1.3 Flow.....	4
1.3.1 Types of Flow.....	4
1.3.2 Peristaltic flow.....	4
1.3.3 Uniform flow.....	4
1.3.4 Non uniform flow.....	4
1.4 Magnetic field	4
1.4.1 Magnetohydrodynamics (MHD).....	5
1.4.2 Maxwell's equations	5
1.5 Physical explanation of dimensionless numbers.....	6
1.5.1 Reynolds number (Re)	6
1.5.2 Grashof's number	6
2 Interaction of nanoparticles for the peristaltic flow in an asymmetric channel with the induced magnetic field	7
2.1 Mathematical formulation.....	7
2.2 Solution of the problem.....	11
2.3 Results and discussion.....	22
2.4 Conclusion.....	37
3 Nanofluid containing Cu – H₂O treated through Maxwell model with induced magnetic field in peristaltic	39
3.1 Mathematical formulation.....	39
3.2 Solution of the problem.....	41
3.3 Results and discussion.....	52

3.4 Conclusion	66
References	68

Chapter 1

Preliminaries

This chapter includes some fundamental definitions which may be useful for the better understanding of the next two chapters.

1.1 Definition

1.1.1 Fluid

Any substance which shows resistance to its internal molecular structure when external force applies. Liquids and gases are identified as fluid since they deform continuously in response to shear stress.

1.1.2 Peristalsis

Peristalsis is a mechanism of fluid that flows through movement of contraction/expansion on the tube/channel walls.

1.1.3 Peristaltic transport

Peristaltic transport is a form of fluid transport generated by a progressive wave of area contraction or expansion along the length of a distensible tube containing fluid.

1.2 Types of fluid

1.2.1 Nanofluid

A nanofluid is a fluid containing nanometre-sized particles. These fluids are engineered colloidal suspensions of nanoparticles in a base conducting fluid. The nanoparticles used in nanofluids are usually made of metals, oxides, carbides and carbon nanotubes.

1.2.1 Newtonian fluid

Such fluid which obeys Newton's law of viscosity is called Newtonian fluid. Newton's law of viscosity is given by

$$\tau = \mu \frac{du}{dy}, \quad (1.1)$$

where, τ is the shear stress, μ is the viscosity of fluid, du/dy is the shear rate or velocity gradient. Gases and most common liquids are tend to Newtonian fluids. Most common examples are Water, thin motor oil, air, sugar solutions, silicone, etc.

1.2.2 Non-Newtonian fluid

Fluid which do not obey the Newton's law of viscosity is called non-Newtonian fluid. Common examples are paints, flour dough, coal tar, ketchup, shampoo, chewing gum and fruit juice.

1.3 Flow

The continuous action or fact of moving of something.

1.3.1 Types of flow

1.3.2 Peristaltic flow

A peristaltic pump is a type of positive displacement pump used for pumping a variety of fluids. The fluid is contained within a flexible tube fitted inside a circular pump casing (though linear peristaltic pumps have been made). A rotor with a number of "rollers", "shoes", "wipers", or "lobes" attached to the external circumference of the rotor compresses the flexible tube. As the rotor turns, the part of the tube under compression is pinched closed thus forcing the fluid to be pumped to move through the tube. Additionally, as the tube opens to its natural state after the passing of the cam ("restitution" or "resilience") fluid flow is induced to the pump. This process is called peristalsis and is used in many biological systems such as the gastrointestinal tract.

1.3.3 Uniform flow

If the flow velocity the same magnitude and direction at every point in the fluid it is said to be uniform.

1.3.4 Non Uniform flow

If at a given instant, the velocity is not the same at every point the flow is non-uniform

1.4 Magnetic field

A magnetic field is the magnetic effect of electric currents and magnetic materials. The term is used for two distinct but closely related fields denoted by the symbols **B** and **H**, where **H** is measured in units of amperes per meter (symbol: $A \cdot m^{-1}$ or A/m) in the SI. **B** is measured in tesla and newton per meter per ampere (symbol: $N \cdot m^{-1} \cdot A^{-1}$ in

the SI. \mathbf{B} is most commonly defined in terms of the Lorentz force it exerts on moving electric charges.

1.4.1 Magnetohydrodynamics (MHD)

Magneto hydro dynamics (MHD) (magneto fluid dynamics or hydro magnetics) is the study of the magnetic properties of electrically conducting fluids. Examples of such magneto-fluids include plasmas, liquid metals, and salt water or electrolytes. The word magneto hydro dynamics (MHD) is derived from magneto-meaning magnetic field, hydro- meaning water, and dynamics meaning movement. The field of MHD was initiated by Hannes Alfvén, for which he received the Nobel Prize in Physics in 1970.

The fundamental concept behind MHD is that magnetic fields can induce currents in a moving conductive fluid, which in turn polarizes the fluid and reciprocally changes the magnetic field itself. The set of equations that describe MHD are a combination of the Navier-Stokes equations of fluid dynamics and Maxwell's equations of electromagnetism. These differential equations must be solved simultaneously, either analytically or numerically.

1.4.2 Maxwell's equations

The Maxwell's equations are the set of four fundamental equations governing electromagnetism, i.e., the behavior of electric and magnetic fields. They were first written down in complete form by James Clerk Maxwell. For the varying fields the differential form of those equations in MKS are given as

$$\left. \begin{aligned} \nabla \cdot \vec{H} &= 0, \\ \nabla \cdot \vec{E} &= \frac{\rho}{\epsilon_0}, \\ \nabla \times \vec{E} &= -\mu_e \frac{\partial \vec{H}}{\partial t}, \\ \nabla \times \vec{H} &= \vec{J}, \\ \vec{J} &= \sigma \left\{ \vec{E} + \mu_e (\nabla \times \vec{H}) \right\}, \end{aligned} \right\} \quad (1.2)$$

where \vec{E} is the electric field, \vec{H} is the magnetic field, \vec{J} is the charge density, $\epsilon_0 = 8.854187817 \times 10^{-12} \text{ Fm}^{-1}$ is the permittivity of free space and $\mu_e = 1.2566370614 \times 10^{-6} \text{ NA}^{-2}$ is the magnetic permeability.

1.5 Physical explanation of dimensionless numbers

1.5.1 Reynolds number (Re)

This dimensionless quantity estimates the correspondence of inertial forces by viscous forces. Reynolds number is used to characterize fluid behavior in the boundary layer flow. Mathematically, it is given by

$$\text{Re} = \frac{\rho u^2 / l}{\mu u / l^2} = \frac{\rho l u}{\mu} \quad (1.3)$$

where u is the fluid velocity, l is the characteristic length and ν is the kinematic viscosity. Laminar flow is characterized by low Reynolds numbers (Dominance of viscous forces) whereas turbulent flow is characterized by high Reynolds numbers (Dominance of inertial forces).

1.5.2 Grashof's number

A dimensionless number represented by Gr in fluid dynamics and heat transfer which approximates the ratio of the buoyancy to viscous force acting on a fluid. It frequently arises in the study of situations involving natural convection. It is named after the German engineer Franz Grashof.

Chapter 2

Interaction of nanoparticles for the peristaltic flow in an asymmetric channel with the induced magnetic field

The present chapter is the review work of [18] on interaction of copper nanoparticle with the base fluid water in an asymmetric channel with the presence of induced magnetic field. The equations describing the flow of nanofluid is simplified by applying the low Reynolds number and long wavelength approximations. The exact solutions of the resulting equations are found. The obtained expressions for velocity and temperature phenomenon are sketched through graphs. The resulting relations for pressure gradient and pressure rise are plotted for various pertinent parameters. The streamlines are drawn for some physical quantities to discuss the trapping phenomenon.

2.1 Mathematical formulation

This section discusses an incompressible peristaltic flow of copper nanofluid in an irregular channel with channel with $d_1 + d_2$. Asymmetry in the flow is because of propagation of peristaltic waves of different amplitudes and phases on the channel walls. An external transverse uniform constant magnetic field \vec{H}_0 , induced magnetic field $\vec{H}(h_x(X, Y, t), \vec{H}_0 + h_y(X, Y, t), 0)$ and the total magnetic field $\vec{H}^+(h_x(X, Y, t), H_0 + h_y(X, Y, t), 0)$ are taken into account. Finally the channel walls are considered to be nonconductive sinusoidal wave propagating beside the walls of the channel with continuous haste c_1 . Disproportionate in the canal flow is reserved due to the subsequent hedge surfaces terminology:

$$\left. \begin{aligned} Y = \bar{H}_1 &= d_1 + a_1 \cos \left[\frac{2\pi}{\lambda} (\bar{X} - c_1 \bar{t}) \right], \\ Y = \bar{H}_2 &= -d_2 - b_1 \cos \left[\frac{2\pi}{\lambda} (\bar{X} - c_1 \bar{t}) + \omega \right] \end{aligned} \right\} \quad (2.1)$$

In the above equations a_1 and b_1 denote the waves amplitudes, λ is the wave length, $d_1 + d_2$ is the channel width, c_1 is the wave speed, \bar{t} is the time, \bar{X} is the direction of wave propagation and Y is perpendicular to \bar{X} . Equations of continuity, equation of motion, equation of energy and Maxwell's equations governing the flow and temperature in the presence of heat source or heat sink which governs the MHD flow are given as

$$\bar{\nabla} \cdot \bar{V} = 0, \quad (2.2)$$

$$\rho_{nf} \left(\frac{\partial \bar{V}}{\partial t} + \bar{V} \cdot \bar{\nabla} \bar{V} \right) = -\bar{\nabla} \bar{p} + \mu_{nf} (\bar{\nabla} \cdot \bar{\nabla} \bar{V}) + (\rho\beta)_{nf} g\alpha (T - T_0) - \bar{\nabla} \left(\frac{1}{2} \mu_e (\bar{H})^2 \right) - \mu_e (\bar{H} \cdot \bar{\nabla}) \bar{H}, \quad (2.3)$$

$$(\rho c)_{nf} \left(\frac{\partial T}{\partial t} + \bar{\nabla} \cdot \bar{\nabla} T \right) = \bar{\nabla} \cdot k_{nf} \bar{\nabla} T + Q_0 (T - T_\infty), \quad (2.4)$$

$$\bar{\nabla} \cdot \bar{H} = 0, \quad \bar{\nabla} \cdot \bar{E} = 0, \quad (2.5)$$

$$\bar{\nabla} \times \bar{H} = \bar{J}, \quad \bar{J} = \sigma \left\{ \bar{E} + \mu_e (\bar{\nabla} \times \bar{H}) \right\}, \quad (2.6)$$

$$\bar{\nabla} \times \bar{E} = -\mu_e \frac{\partial \bar{H}}{\partial t}. \quad (2.7)$$

Combining Eqs. (2.5) to (2.7) we obtain the induction equation (2.8) as follows

$$\frac{\partial \bar{H}}{\partial t} = \bar{\nabla} \times \left(\bar{\nabla} \times \bar{H} \right) + \frac{1}{\xi} \nabla^2 \bar{H}, \quad (2.8)$$

where $\xi = \sigma \mu_e$ is the magnetic diffusivity, σ is the electrical conductivity, μ_e is magnetic permeability, ρ_{nf} is the effective density of the incompressible nano fluid, $(\rho c)_{nf}$ is the heat capacity of the nanofluid, $(\rho c)_p$ gives effective heat capacity of the nano particle material, k_{nf} implies effective thermal conductivity of nanofluid, g stands for constant of gravity, μ_{nf} is the effective viscosity of the fluid, d/dt gives the material time derivative, \bar{p} is the pressure. The appearance for static and wave structures are connected by the subsequent associations

$$x = X - ct, \quad y = Y, \quad u = U - c, \quad v = V. \quad (2.9)$$

The dimensionless parameters used in the problem are defined as follow

$$\begin{aligned}
\bar{p} &= \frac{a^2}{\mu_f c \lambda} p, \quad \bar{u} = \frac{\lambda}{ac} u, \quad \bar{v} = \frac{v}{c}, \quad \bar{y} = \frac{y}{\lambda}, \quad \bar{x} = \frac{x}{a}, \quad \bar{t} = \frac{c}{\lambda} t, \\
\omega &= \frac{b}{a}, \quad \text{Re} = \frac{\rho c a}{\mu_f}, \quad \delta = \frac{a}{\lambda}, \quad \bar{\theta} = \frac{T - T_0}{T_1 - T_0}, \quad \bar{\Phi} = \frac{\Phi}{H_0 a}, \\
\bar{\psi} &= \frac{\psi}{ca}, \quad R_m = \sigma \mu_e ac, \quad \bar{h}_x = \bar{\Phi}_x, \quad G_r = \frac{\rho_f g \alpha a^2}{\lambda \mu_f c} (T_1 - T_0), \\
S_1 &= \frac{\bar{H}_0}{c} \sqrt{\frac{\mu_e}{\rho}}, \quad \alpha_{nf} = \frac{k}{(\rho c)_f}, \quad \tau = \frac{(\rho c)_r}{(\rho c)_f}, \quad \bar{h}_y = -\bar{\Phi}_y.
\end{aligned} \tag{2.10}$$

After using the above non-dimensional parameters and transformation in Eq. (2.9) employing the assumptions of long wavelength ($\delta \rightarrow 0$), the dimensionless governing equations (without using bars) for nanofluid in the wave frame take the final form as

$$\frac{\partial u}{\partial x} + \frac{\partial v}{\partial y} = 0, \tag{2.11}$$

$$\frac{dp}{dx} = \frac{\partial^3 \psi}{\partial y^3} \left(\frac{1}{(1-\phi)^{2.5}} \right) + \text{Re} S_1^2 \Phi_{yy} + \frac{(\rho\beta)_{nf}}{(\rho\beta)_f} Gr \theta, \tag{2.12}$$

$$\frac{dp}{dy} = 0, \tag{2.13}$$

$$\Phi_{yy} = R_m \left(E - \frac{\partial \psi}{\partial y} \right), \tag{2.14}$$

$$\frac{\partial^2 \theta}{\partial y^2} + \theta \frac{k_f}{k_{nf}} Q_0 = 0. \tag{2.15}$$

Putting Eq. (2.14) into Eq. (2.12), we get

$$\frac{dp}{dx} = \frac{\partial^3 \psi}{\partial y^3} \left(\frac{1}{(1-\phi)^{2.5}} \right) + \text{Re} S_1^2 R_m \left(E - \frac{\partial \psi}{\partial y} \right) + \frac{(\rho\beta)_{nf}}{(\rho\beta)_f} Gr \theta, \tag{2.16}$$

Taking derivative of above equation with respect to y , we have

$$\frac{\partial^4 \psi}{\partial y^4} \left(\frac{1}{(1-\phi)^{2.5}} \right) + \text{Re} S_1^2 R_m \left(-\frac{\partial^2 \psi}{\partial y^2} \right) + \frac{(\rho\beta)_{nf}}{(\rho\beta)_f} Gr \frac{\partial \theta}{\partial y} = 0. \tag{2.17}$$

The non-dimensional boundaries will take the form as

$$\psi = \frac{F}{2}, \quad \frac{\partial \psi}{\partial y} = -1, \quad \text{at} \quad y = h_1, \quad (2.18)$$

$$\psi = -\frac{F}{2}, \quad \frac{\partial \psi}{\partial y} = -1, \quad \text{at} \quad y = h_2, \quad (2.19)$$

$$\theta = 0 \quad \text{at} \quad y = h_1, \quad \theta = 1 \quad \text{at} \quad y = h_2, \quad (2.20)$$

$$\Phi = 0 \quad \text{at} \quad y = h_1, \quad \Phi = 0 \quad \text{at} \quad y = h_2. \quad (2.21)$$

The pressure rise Δp , axial induced magnetic h_x and current density j_z in non-dimensional form is defined as

$$\Delta p = \int_0^1 \frac{dp}{dx} dx, \quad (2.22)$$

$$h_x = \frac{\partial \Phi}{\partial y}, \quad (2.23)$$

$$j_z = \frac{\partial h_x}{\partial y}. \quad (2.24)$$

The effective density ρ_{nf} , the effective dynamic viscosity μ_{nf} and the thermal diffusibility α_{nf} of the nanofluid, are defined as

$$\rho_{nf} = (1-\phi)\rho_f + \phi\rho_s, \quad \mu_{nf} = \frac{\mu_f}{(1-\phi)^{2.5}},$$

$$(\rho c_p)_{nf} = (1-\phi)(\rho c_p)_f + \phi(\rho c_p)_s, \quad \alpha_{nf} = \frac{k_{nf}}{(\rho c_p)_{nf}}, \quad (2.25)$$

$$k_{nf} = k_f \left(\frac{k_s + 2k_f - 2\phi(k_f - k_s)}{k_s + 2k_f + \phi(k_f - k_s)} \right).$$

Here, ϕ is the solid volume fraction, μ_f is the dynamic viscosity of basic fluid, ρ_f , ρ_s are the densities of basic fluid and nanoparticle respectively, k_{nf} is the thermal conductivity and $(\rho c_p)_{nf}$ is the heat capacity of nanofluid. Thermal physical properties of water and nanoparticles are defined as [19, 20].

Table 2.1. Thermal-physical properties of water and nanoparticles

Physical Properties	Water(H_2O)	Copper(Cu)
$\rho(kgm^{-3})$	997.1	8933
C_p	4179	385
$\beta \times 10^5 (K^{-1})$	21	1.67
$k, Wm^{-1} (K^{-1})$	0.613	401

2.2 Solution of the problem

The exact solutions of Eqs. (2.14), (2.15) and (2.17) subject to boundary conditions (2.18) to (2.21) are found as follows:

$$\theta(y) = C_3 \cos y\sqrt{C_1} + C_2 \sin y\sqrt{C_1}, \quad (2.26)$$

$$\psi(y) = \left. \begin{aligned} & \frac{\cos y\sqrt{C_1}C_2C_6}{\sqrt{C_1}(C_1C_4 + C_5)} + \frac{\sin y\sqrt{C_1}C_3C_6}{\sqrt{C_1}(C_1C_4 + C_5)} + \frac{1}{C_5} \left(\begin{aligned} & \cosh\left(\frac{y\sqrt{C_5}}{\sqrt{C_4}}\right) \\ & -\sinh\left(\frac{y\sqrt{C_5}}{\sqrt{C_4}}\right) \end{aligned} \right) \\ & C_4(C_7 + \cosh\left(\frac{2y\sqrt{C_5}}{\sqrt{C_4}}\right)C_8 + \sinh\left(\frac{2y\sqrt{C_5}}{\sqrt{C_4}}\right)C_8) + C_9 + yC_{10} \end{aligned} \right\}, \quad (2.27)$$

$$\Phi(y) = \left. \begin{aligned} & \frac{1}{2C_1C_5^{3/2}(C_1C_4 + C_5)} \\ & \left(\begin{aligned} & 2R_m \sin(y\sqrt{C_1})C_2C_5^{3/2}C_6 + 2R_m \cos(y\sqrt{C_1}) \\ & \left(\begin{aligned} & 2R_m \left(\cosh\left(\frac{y\sqrt{C_5}}{\sqrt{C_4}}\right) - \sinh\left(\frac{y\sqrt{C_5}}{\sqrt{C_4}}\right) \right) \\ & \left(\begin{aligned} & C_7 - \cosh\left(\frac{2y\sqrt{C_5}}{\sqrt{C_4}}\right)C_8 - \\ & \sinh\left(\frac{2y\sqrt{C_5}}{\sqrt{C_4}}\right)C_8 \end{aligned} \right) \end{aligned} \right) + \\ & C_5^{3/2}(ER_m y^2 - R_m y^2 C_{10} + 2C_{11} + 2yC_{12}) \end{aligned} \right) \end{aligned} \right\}. \quad (2.28)$$

The mean volume flow rate Q over one period is given as

$$Q = F + 1 + d. \quad (2.29)$$

The pressure gradient dp/dx axial induced magnetic h_1 and current density j_z are elaborated as

$$\frac{dp}{dx} = \left. \begin{aligned} & C_{20} - \frac{1}{C_1 C_4 + C_5} \left(C_1 C_4 + C_5 + \sin \sqrt{C_1} h_2 C_2 C_6 + \cos \sqrt{C_1} h_2 C_3 C_6 \right) - \\ & \left(e^{-\frac{\sqrt{C_5} h_1}{\sqrt{C_4}} - \frac{\sqrt{C_5} h_2}{\sqrt{C_4}}} \left(e^{\frac{\sqrt{C_5} h_1}{\sqrt{C_4}}} + e^{\frac{\sqrt{C_5} h_2}{\sqrt{C_4}}} \right) \sqrt{C_4} C_{19} \right) \\ & \sqrt{C_5} \left(\begin{aligned} & \frac{4C_4^{3/2}}{C_5^{3/2}} - \frac{2e^{\frac{\sqrt{C_5} h_1}{\sqrt{C_4}} - \frac{\sqrt{C_5} h_2}{\sqrt{C_4}}} C_4^{3/2}}{C_5^{3/2}} - \\ & \frac{2e^{-\frac{\sqrt{C_5} h_1}{\sqrt{C_4}} + \frac{\sqrt{C_5} h_2}{\sqrt{C_4}}} C_4^{3/2}}{C_5^{3/2}} + \frac{e^{\frac{\sqrt{C_5} h_1}{\sqrt{C_4}} - \frac{\sqrt{C_5} h_2}{\sqrt{C_4}}} C_4 h_1}{C_5} - \\ & e^{\frac{\sqrt{C_5} h_1}{\sqrt{C_4}} + \frac{\sqrt{C_5} h_2}{\sqrt{C_4}}} C_4 h_1 - e^{\frac{\sqrt{C_5} h_1}{\sqrt{C_4}} - \frac{\sqrt{C_5} h_2}{\sqrt{C_4}}} C_4 h_2 + \\ & \frac{e^{-\frac{\sqrt{C_5} h_1}{\sqrt{C_4}} + \frac{\sqrt{C_5} h_2}{\sqrt{C_4}}} C_4 h_2}{C_5} \end{aligned} \right) \end{aligned} \right\} \quad (2.30)$$

$$h_1 = \frac{1}{\sqrt{C_1 C_5 (C_1 C_4 + C_5)}} \left(\begin{array}{l} R_m \cos y \sqrt{C_1} C_2 C_5 C_6 - R_m \sin y \sqrt{C_1} C_3 C_5 C_6 + \\ \left(\begin{array}{l} ER_m y C_5 - R_m \left(\begin{array}{l} \cosh \left(\frac{y \sqrt{C_5}}{\sqrt{C_4}} \right) \\ - \sinh \frac{y \sqrt{C_5}}{\sqrt{C_4}} \end{array} \right) \\ \left(\begin{array}{l} C_7 + \cosh \left(\frac{2y \sqrt{C_5}}{\sqrt{C_4}} \right) C_8 \\ + \sinh \left(\frac{2y \sqrt{C_5}}{\sqrt{C_4}} \right) C_8 \end{array} \right) \\ -R_m y C_5 C_{10} + C_5 C_{12} \end{array} \right) \end{array} \right) \quad (2.31)$$

$$J_1 = \left. \begin{array}{l} \frac{ER_m C_1 C_4}{C_1 C_4 + C_5} + \frac{ER_m C_5}{C_1 C_4 + C_5} - \frac{R_m \sin y \sqrt{C_1} C_2 C_6}{C_1 C_4 + C_5} - \frac{R_m \cos y \sqrt{C_1} C_3 C_6}{C_1 C_4 + C_5} \\ + \frac{R_m \cosh \left(\frac{y \sqrt{C_5}}{\sqrt{C_4}} \right) \sqrt{C_4} C_7}{\sqrt{C_5}} - \frac{R_m \sinh \left(\frac{y \sqrt{C_5}}{\sqrt{C_4}} \right) \sqrt{C_4} C_7}{\sqrt{C_5}} \\ - \frac{R_m \cosh \left(\frac{y \sqrt{C_5}}{\sqrt{C_4}} \right) \sqrt{C_4} C_8}{\sqrt{C_5}} - \frac{R_m \sinh \left(\frac{y \sqrt{C_5}}{\sqrt{C_4}} \right) \sqrt{C_4} C_8}{\sqrt{C_5}} \\ - \frac{R_m C_1 C_4 C_{10}}{C_1 C_4 + C_5} - \frac{R_m C_5 C_{10}}{C_1 C_4 + C_5} \end{array} \right\} \quad (2.32)$$

The constants $C_1 - C_{23}$ are evaluated using Mathematica 9.

$$C_1 = \frac{k_1 Q_0}{k_n} \quad (2.33)$$

$$C_2 = \frac{\cos \sqrt{C_1} h_1}{-\cos \sqrt{C_1} h_2 \sin \sqrt{C_1} h_1 + \cos \sqrt{C_1} h_1 \sin \sqrt{C_1} h_2} \quad (2.34)$$

$$C_3 = \frac{\sin \sqrt{C_1} h_1}{\cos \sqrt{C_1} h_2 \sin \sqrt{C_1} h_1 - \cos \sqrt{C_1} h_1 \sin \sqrt{C_1} h_2} \}, \quad (2.35)$$

$$C_4 = \frac{1}{(1-\phi)^{2.5}}, \quad (2.36)$$

$$C_5 = ReS_1^2 R_m, \quad (2.37)$$

$$C_6 = \frac{(\rho\beta)_{nf}}{(\rho\beta)_l} Gr, \quad (2.38)$$

$$C_7 = \frac{\left(\begin{array}{c} \sin \sqrt{C_1} h_1 C_2 C_6 - \sin \sqrt{C_1} h_2 C_2 C_6 + \cos \sqrt{C_1} h_1 C_3 C_6 \\ C_1 C_4 + C_5 \quad C_1 C_4 + C_5 \quad C_1 C_4 + C_5 \\ - \cos \sqrt{C_1} h_2 C_3 C_6 \\ C_1 C_4 + C_5 \end{array} \right) C_{13}}{C_{14}} \}, \quad (2.39)$$

$$C_8 = \left(\frac{\left(\sin \sqrt{C_1} h_1 C_2 - \sin \sqrt{C_1} h_2 C_2 + \cos \sqrt{C_1} h_1 C_3 - \cos \sqrt{C_1} h_2 C_3 \right)}{\sqrt{C_5} C_6} + \frac{\left(\left(e^{\frac{\sqrt{C_5} h_1}}{\sqrt{C_4}} - e^{\frac{\sqrt{C_5} h_2}}{\sqrt{C_4}}} \right) \sqrt{C_4} (C_1 C_4 + C_5) \right)}{\left(\frac{e^{\frac{\sqrt{C_5} h_1}}{\sqrt{C_4}} \sqrt{C_4}} + e^{\frac{\sqrt{C_5} h_2}}{\sqrt{C_4}} \sqrt{C_4}} \right)} \right) C_{15} \left(\frac{\left(e^{\frac{\sqrt{C_5} h_1}}{\sqrt{C_4}} \sqrt{C_4} - e^{\frac{\sqrt{C_5} h_2}}{\sqrt{C_4}} \sqrt{C_4}} \right)}{\sqrt{C_5}} \right) C_{16} \}, \quad (2.40)$$

$$C_9 = C_{17} - \left(\begin{array}{c} \left(e^{\frac{\sqrt{C_5} h_1}{\sqrt{C_4}} \frac{\sqrt{C_5} h_2}{\sqrt{C_4}}} \sqrt{C_4} C_{18} \begin{pmatrix} -e^{\frac{\sqrt{C_5} h_1}{\sqrt{C_4}}} \sqrt{C_4} + e^{\frac{\sqrt{C_5} h_2}{\sqrt{C_4}}} \sqrt{C_4} \\ -e^{\frac{\sqrt{C_5} h_1}{\sqrt{C_4}}} \sqrt{C_5} h_2 \\ -e^{\frac{\sqrt{C_5} h_2}{\sqrt{C_4}}} \sqrt{C_5} h_2 \end{pmatrix} \right) \\ \left(\begin{array}{c} \frac{4C_4^{3/2}}{C_5^{3/2}} - \frac{2e^{\frac{\sqrt{C_5} h_1}{\sqrt{C_4}} \frac{\sqrt{C_5} h_2}{\sqrt{C_4}}} C_4^{3/2}}{C_5^{3/2}} - \frac{2e^{\frac{\sqrt{C_5} h_1}{\sqrt{C_4}} + \frac{\sqrt{C_5} h_2}{\sqrt{C_4}}} C_4^{3/2}}{C_5^{3/2}} \\ C_5 + \frac{e^{\frac{\sqrt{C_5} h_1}{\sqrt{C_4}} \frac{\sqrt{C_5} h_2}{\sqrt{C_4}}} C_4 h_1}{C_5} - \frac{e^{\frac{\sqrt{C_5} h_1}{\sqrt{C_4}} + \frac{\sqrt{C_5} h_2}{\sqrt{C_4}}} C_4 h_1}{C_5} - \frac{e^{\frac{\sqrt{C_5} h_1}{\sqrt{C_4}} \frac{\sqrt{C_5} h_2}{\sqrt{C_4}}} C_4 h_2}{C_5} \\ + \frac{e^{\frac{\sqrt{C_5} h_1}{\sqrt{C_4}} + \frac{\sqrt{C_5} h_2}{\sqrt{C_4}}} C_4 h_2}{C_5} \end{array} \right) \end{array} \right) \quad (2.41)$$

$$C_{20} - \frac{1}{C_1 C_4 + C_5} \left(C_1 C_4 + C_5 + \sin \sqrt{C_1} h_2 C_2 C_6 + \cos \sqrt{C_1} h_2 C_3 C_6 \right) - \left(e^{\frac{\sqrt{C_5} h_1}{\sqrt{C_4}} \frac{\sqrt{C_5} h_2}{\sqrt{C_4}}} \left(e^{\frac{\sqrt{C_5} h_1}{\sqrt{C_4}}} + e^{\frac{\sqrt{C_5} h_2}{\sqrt{C_4}}} \right) \sqrt{C_4} C_{19} \right)$$

$$C_{10} = \left(\begin{array}{c} \left(\begin{array}{c} \frac{4C_4^{3/2}}{C_5^{3/2}} - \frac{2e^{\frac{\sqrt{C_5} h_1}{\sqrt{C_4}} \frac{\sqrt{C_5} h_2}{\sqrt{C_4}}} C_4^{3/2}}{C_5^{3/2}} \\ 2e^{\frac{\sqrt{C_5} h_1}{\sqrt{C_4}} + \frac{\sqrt{C_5} h_2}{\sqrt{C_4}}} C_4^{3/2} + \frac{e^{\frac{\sqrt{C_5} h_1}{\sqrt{C_4}} \frac{\sqrt{C_5} h_2}{\sqrt{C_4}}} C_4 h_1}{C_5} - \frac{e^{\frac{\sqrt{C_5} h_1}{\sqrt{C_4}} + \frac{\sqrt{C_5} h_2}{\sqrt{C_4}}} C_4 h_1}{C_5} \\ \frac{\sqrt{C_5} h_1}{\sqrt{C_4}} \frac{\sqrt{C_5} h_2}{\sqrt{C_4}} C_4 h_2 + \frac{e^{\frac{\sqrt{C_5} h_1}{\sqrt{C_4}} + \frac{\sqrt{C_5} h_2}{\sqrt{C_4}}} C_4 h_2}{C_5} \end{array} \right) \end{array} \right) \quad (2.42)$$

$$C_{11} = -\frac{1}{-h_1 + h_2} \left(C_{21} h_2 - h_1 \left(\begin{array}{l} \left(\frac{R_m \sin \sqrt{C_1} h_2 C_2 C_6}{C_1 (C_1 C_4 + C_5)} + \frac{R_m \cos \sqrt{C_1} h_2 C_3 C_6}{C_1 (C_1 C_4 + C_5)} \right. \right. \\ \left. \left. + \frac{1}{C_5^{3/2}} R_m \left(\cosh \left(\frac{\sqrt{C_5} h_2}{\sqrt{C_4}} \right) - \sinh \left(\frac{\sqrt{C_5} h_2}{\sqrt{C_4}} \right) \right) \right) \right. \\ \left. C_4^{3/2} \left(\begin{array}{l} C_7 - \cosh \left(\frac{2\sqrt{C_5} h_2}{\sqrt{C_4}} \right) C_8 - \\ \sinh \left(\frac{2\sqrt{C_5} h_2}{\sqrt{C_4}} \right) C_8 \end{array} \right) + \frac{1}{2} E R_m h_2^2 \right. \\ \left. \left. - \frac{1}{2} R_m C_{10} h_2^2 \right) \right) \right) \quad (2.43)$$

$$C_{12} = \left(\begin{array}{l} -\frac{1}{h_2} C_{22} + \frac{1}{h_2 (-h_1 + h_2)} \\ \left(\begin{array}{l} \left(\frac{R_m \sin \sqrt{C_1} h_1 C_2 C_6}{C_1 (C_1 C_4 + C_5)} + \frac{R_m \cos \sqrt{C_1} h_1 C_3 C_6}{C_1 (C_1 C_4 + C_5)} \right. \right. \\ \left. \left. + \frac{1}{C_5^{3/2}} R_m \left(\cosh \left(\frac{\sqrt{C_5} h_1}{\sqrt{C_4}} \right) - \sinh \left(\frac{\sqrt{C_5} h_1}{\sqrt{C_4}} \right) \right) \right) C_4^{3/2} \right. \\ \left(\begin{array}{l} C_7 - \cosh \left(\frac{2\sqrt{C_5} h_1}{\sqrt{C_4}} \right) C_8 \\ - \sinh \left(\frac{2\sqrt{C_5} h_1}{\sqrt{C_4}} \right) C_8 \end{array} \right) + \frac{1}{2} E R_m h_1^2 - \frac{1}{2} R_m C_{10} h_1^2 \end{array} \right) h_2 - h_1 C_{23} \end{array} \right) \quad (2.44)$$

$$C_{13} = \left(\begin{array}{l} \left(\frac{e^{\frac{\sqrt{C_5} h_1}{\sqrt{C_4}}} C_4}{C_5} - \frac{e^{\frac{\sqrt{C_5} h_2}{\sqrt{C_4}}} C_4}{C_5} - \frac{e^{\frac{\sqrt{C_5} h_2}{\sqrt{C_4}}} \sqrt{C_4} (h_1 - h_2)}{\sqrt{C_5}} \right) + \left(\frac{e^{\frac{\sqrt{C_5} h_1}{\sqrt{C_4}}} \sqrt{C_4}}{\sqrt{C_5}} - \frac{e^{\frac{\sqrt{C_5} h_2}{\sqrt{C_4}}} \sqrt{C_4}}{\sqrt{C_5}} \right) \\ -F \left(\frac{\cos \sqrt{C_1} h_1 C_2 C_6}{\sqrt{C_1} (C_1 C_4 + C_5)} + \frac{\cos \sqrt{C_1} h_2 C_2 C_6}{\sqrt{C_1} (C_1 C_4 + C_5)} + \frac{\sin \sqrt{C_1} h_1 C_3 C_6}{\sqrt{C_1} (C_1 C_4 + C_5)} - \right. \\ \left. \frac{\sin \sqrt{C_1} h_2 C_3 C_6}{\sqrt{C_1} (C_1 C_4 + C_5)} - \left(1 + \frac{\sin \sqrt{C_1} h_2 C_2 C_6}{C_1 C_4 + C_5} + \frac{\cos \sqrt{C_1} h_2 C_3 C_6}{C_1 C_4 + C_5} \right) (h_1 - h_2) \right) \end{array} \right) \quad (2.45)$$

$$C_{14} = \left\{ \begin{array}{l} \frac{4C_4^{3,2}}{C_5^{3,2}} - \frac{2e^{\frac{\sqrt{C_1}h_1}{\sqrt{C_4}} \frac{\sqrt{C_1}h_2}{\sqrt{C_4}}} C_4^{3,2}}{C_5^{3,2}} - \frac{2e^{\frac{\sqrt{C_1}h_1}{\sqrt{C_4}} \frac{\sqrt{C_1}h_2}{\sqrt{C_4}}} C_4^{3,2}}{C_5^{3,2}} + \frac{e^{\frac{\sqrt{C_1}h_1}{\sqrt{C_4}} \frac{\sqrt{C_1}h_2}{\sqrt{C_4}}} C_4 h_1}{C_5} \\ \frac{e^{\frac{\sqrt{C_1}h_1}{\sqrt{C_4}} \frac{\sqrt{C_1}h_2}{\sqrt{C_4}}} C_4 h_1}{C_5} - \frac{e^{\frac{\sqrt{C_1}h_1}{\sqrt{C_4}} \frac{\sqrt{C_1}h_2}{\sqrt{C_4}}} C_4 h_2}{C_5} + \frac{e^{\frac{\sqrt{C_1}h_1}{\sqrt{C_4}} \frac{\sqrt{C_1}h_2}{\sqrt{C_4}}} C_4 h_2}{C_5} \end{array} \right\}, \quad (2.46)$$

$$C_{15} = \frac{1}{C_5(C_1 C_4 + C_5)} \sqrt{C_4} \left\{ \begin{array}{l} \frac{-1}{(\sqrt{C_1})} \left(e^{\frac{\sqrt{C_1}h_1}{\sqrt{C_4}}} - e^{\frac{\sqrt{C_1}h_2}{\sqrt{C_4}}} \right) \\ \left(\begin{array}{l} \left(\begin{array}{l} \left(\sin \sqrt{C_1} h_1 \right) C_2 \\ - \left(\sin \sqrt{C_1} h_2 \right) C_2 \end{array} \right) \\ + \left(\begin{array}{l} \left(\cos \sqrt{C_1} h_1 \right) C_3 \\ - \left(\cos \sqrt{C_1} h_2 \right) C_3 \end{array} \right) \end{array} \right) \\ C_6 \left(\begin{array}{l} -e^{\frac{\sqrt{C_1}h_1}{\sqrt{C_4}}} \sqrt{C_4} \\ + e^{\frac{\sqrt{C_1}h_2}{\sqrt{C_4}}} \left(\sqrt{C_4} \right. \\ \left. + \sqrt{C_5} (h_1 - h_2) \right) \end{array} \right) \\ \left(\begin{array}{l} \left(\left(\cos \sqrt{C_1} h_1 - \cos \sqrt{C_1} h_2 \right) C_2 + \right) C_6 \\ \left(-\sin \sqrt{C_1} h_1 + \sin \sqrt{C_1} h_2 \right) C_3 \end{array} \right) \\ \sqrt{C_5} \left(\begin{array}{l} \left(\begin{array}{l} \left(\sin \sqrt{C_1} h_2 C_2 + \right) \\ \left(\cos \sqrt{C_1} h_2 C_3 \right) \end{array} \right) \\ + \sqrt{C_1} \left(C_6 (h_1 - h_2) + C_1 C_4 (F + h_1 - h_2) \right. \\ \left. + C_5 (F + h_1 - h_2) \right) \end{array} \right) \end{array} \right\}, \quad (2.47)$$

$$C_{16} = \left\{ \begin{array}{l} \frac{4C_4^{3,2}}{C_5^{3,2}} - \frac{2e^{\frac{\sqrt{C_1}h_1}{\sqrt{C_4}} \frac{\sqrt{C_1}h_2}{\sqrt{C_4}}} C_4^{3,2}}{C_5^{3,2}} - \frac{2e^{\frac{\sqrt{C_1}h_1}{\sqrt{C_4}} \frac{\sqrt{C_1}h_2}{\sqrt{C_4}}} C_4^{3,2}}{C_5^{3,2}} + \frac{e^{\frac{\sqrt{C_1}h_1}{\sqrt{C_4}} \frac{\sqrt{C_1}h_2}{\sqrt{C_4}}} C_4 h_1}{C_5} \\ \frac{e^{\frac{\sqrt{C_1}h_1}{\sqrt{C_4}} \frac{\sqrt{C_1}h_2}{\sqrt{C_4}}} C_4 h_1}{C_5} - \frac{e^{\frac{\sqrt{C_1}h_1}{\sqrt{C_4}} \frac{\sqrt{C_1}h_2}{\sqrt{C_4}}} C_4 h_2}{C_5} + \frac{e^{\frac{\sqrt{C_1}h_1}{\sqrt{C_4}} \frac{\sqrt{C_1}h_2}{\sqrt{C_4}}} C_4 h_2}{C_5} \end{array} \right\}, \quad (2.48)$$

$$\left. \begin{aligned}
& \frac{F}{2} + \frac{\cos\sqrt{C_1}h_2C_2C_6}{\sqrt{C_1}(C_1C_4+C_5)} \\
& - \frac{\sin\sqrt{C_1}h_2C_3C_6}{\sqrt{C_1}(C_1C_4+C_5)} + \\
& \left(\frac{C_1C_4+C_5 + \sin\sqrt{C_1}h_2C_2C_6}{+ \cos\sqrt{C_1}h_2C_3C_6} \right) h_2 \\
& \frac{\quad}{C_1C_4+C_5}
\end{aligned} \right\} \quad (2.49)$$

$$C_{17} = \left(\begin{array}{l}
e^{\frac{\sqrt{C_5}h_2}{\sqrt{C_4}}} \left(\begin{array}{l}
\sin\sqrt{C_1}h_1C_2 - \sin\sqrt{C_1}h_2C_2 \\
+ \cos\sqrt{C_1}h_1C_3 \\
- \cos\sqrt{C_1}h_2C_3
\end{array} \right) \\
C_6 \left(-\sqrt{C_4} + \sqrt{C_5}h_2 \right) \\
\left(\begin{array}{cc}
\sqrt{C_5}h_1 & \sqrt{C_5}h_2 \\
e^{\frac{\sqrt{C_5}h_1}{\sqrt{C_4}}} & -e^{\frac{\sqrt{C_5}h_2}{\sqrt{C_4}}}
\end{array} \right) \sqrt{C_5}(C_1C_4+C_5)
\end{array} \right)$$

$$\begin{aligned}
& \frac{1}{C_5(C_1C_4 + C_5)} \sqrt{C_4} \\
& \left(\begin{array}{l} \left(\begin{array}{l} \sin \sqrt{C_1} h_1 \\ -\sin \sqrt{C_1} h_2 \end{array} \right) C_2 \\ + \left(\begin{array}{l} \cos \sqrt{C_1} h_1 \\ -\cos \sqrt{C_1} h_2 \end{array} \right) C_3 \end{array} \right) \\
& C_6 \left(\begin{array}{l} e^{\frac{\sqrt{C_1} h_1}{\sqrt{C_4}}} \sqrt{C_4} \\ -e^{\frac{\sqrt{C_1} h_2}{\sqrt{C_4}}} \left(\sqrt{C_4} + \right. \\ \left. + e^{\frac{\sqrt{C_1} h_1}{\sqrt{C_4}}} \left(\sqrt{C_5} (h_1 - h_2) \right) \right) \end{array} \right) \\
& -1 / (\sqrt{C_1}) \\
C_{18} = & \left(\begin{array}{l} \left(\begin{array}{l} \left(\begin{array}{l} \cos \sqrt{C_1} h_1 \\ -\cos \sqrt{C_1} h_2 \end{array} \right) C_2 \\ + \left(\begin{array}{l} -\sin \sqrt{C_1} h_1 \\ +\sin \sqrt{C_1} h_2 \end{array} \right) C_3 \end{array} \right) \\ \left(e^{\frac{\sqrt{C_5} h_1}{\sqrt{C_4}}} - e^{\frac{\sqrt{C_5} h_2}{\sqrt{C_4}}} \right) \sqrt{C_5} \\ C_6 + \left(\begin{array}{l} \left(\begin{array}{l} \sin \sqrt{C_1} h_2 C_2 \\ +\cos \sqrt{C_1} h_2 C_3 \end{array} \right) \\ \sqrt{C_1} C_6 (h_1 - h_2) \\ + C_1 C_4 (F + h_1 - h_2) \\ + C_5 (F + h_1 - h_2) \end{array} \right) \end{array} \right) \end{array} \right) \quad (2.50)
\end{aligned}$$

$$C_{19} = \left[\begin{array}{l} \left(\begin{array}{l} \frac{\sin \sqrt{C_1} h_1 C_2 C_6}{C_1 C_4 + C_5} \\ \frac{\sin \sqrt{C_1} h_2 C_2 C_6}{C_1 C_4 + C_5} \\ + \frac{\cos \sqrt{C_1} h_1 C_3 C_6}{C_1 C_4 + C_5} \\ \frac{\cos \sqrt{C_1} h_2 C_3 C_6}{C_1 C_4 + C_5} \end{array} \right) \left(\begin{array}{l} \frac{\sqrt{C_3} h_1}{e^{\sqrt{C_4}} C_4} - \frac{\sqrt{C_3} h_2}{e^{\sqrt{C_4}} C_4} \\ \frac{C_5}{C_5} - \frac{C_5}{C_5} \\ - \frac{\sqrt{C_3} h_2}{e^{\sqrt{C_4}} \sqrt{C_4} (h_1 - h_2)} \\ \frac{\sqrt{C_5}}{\sqrt{C_5}} \end{array} \right) \\ + \left(\begin{array}{l} \frac{\sqrt{C_3} h_1}{e^{\sqrt{C_4}} \sqrt{C_4}} \\ \frac{\sqrt{C_5}}{\sqrt{C_5}} \\ - \frac{\sqrt{C_3} h_2}{e^{\sqrt{C_4}} \sqrt{C_4}} \\ \frac{\sqrt{C_5}}{\sqrt{C_5}} \end{array} \right) \left(\begin{array}{l} -F - \frac{\cos \sqrt{C_1} h_1 C_2 C_6}{\sqrt{C_1} (C_1 C_4 + C_5)} \\ + \frac{\cos \sqrt{C_1} h_2 C_2 C_6}{\sqrt{C_1} (C_1 C_4 + C_5)} \\ + \frac{\sin \sqrt{C_1} h_1 C_3 C_6}{\sqrt{C_1} (C_1 C_4 + C_5)} \\ - \frac{\sin \sqrt{C_1} h_2 C_3 C_6}{\sqrt{C_1} (C_1 C_4 + C_5)} \\ \left(1 + \frac{\sin \sqrt{C_1} h_2 C_2 C_6}{C_1 C_4 + C_5} + \frac{\cos \sqrt{C_1} h_2 C_3 C_6}{C_1 C_4 + C_5} \right) (h_1 - h_2) \end{array} \right) \end{array} \right] \quad (2.51)$$

$$C_{20} = \frac{\left(\begin{array}{l} \frac{\sqrt{C_3} h_2}{e^{\sqrt{C_4}}} \left(\sin \sqrt{C_1} h_1 C_2 - \sin \sqrt{C_1} h_2 C_2 + \cos \sqrt{C_1} h_1 C_3 - \right) C_6 \\ \cos \sqrt{C_1} h_2 C_3 \end{array} \right)}{\left(\left(\begin{array}{l} \frac{\sqrt{C_3} h_1}{e^{\sqrt{C_4}}} - \frac{\sqrt{C_3} h_2}{e^{\sqrt{C_4}}} \end{array} \right) (C_1 C_4 + C_5) \right)} \quad (2.52)$$

$$C_{21} = \left\{ \begin{array}{l} \left(\frac{R_m \sin \sqrt{C_1} h_1 C_2 C_6}{C_1 (C_1 C_4 + C_5)} + \frac{R_m \cos \sqrt{C_1} h_1 C_3 C_6}{C_1 (C_1 C_4 + C_5)} + \frac{1}{C_5^{3/2}} R_m \begin{pmatrix} \cosh \left(\frac{\sqrt{C_5} h_1}{\sqrt{C_4}} \right) \\ \sinh \left(\frac{\sqrt{C_5} h_1}{\sqrt{C_4}} \right) \end{pmatrix} \right) \\ C_4^{3/2} \left(C_7 - \cosh \left(\frac{2\sqrt{C_5} h_1}{\sqrt{C_4}} \right) C_8 - \sinh \left(\frac{2\sqrt{C_5} h_1}{\sqrt{C_4}} \right) C_8 \right) + \\ \frac{1}{2} E R_m h_1^2 - \frac{1}{2} R_m C_{10} h_1^2 \end{array} \right\}, \quad (2.53)$$

$$C_{22} = \left\{ \begin{array}{l} \left(\frac{R_m \sin \sqrt{C_1} h_2 C_2 C_6}{C_1 (C_1 C_4 + C_5)} + \frac{R_m \cos \sqrt{C_1} h_2 C_3 C_6}{C_1 (C_1 C_4 + C_5)} + \frac{1}{C_5^{3/2}} R_m \begin{pmatrix} \cosh \left(\frac{\sqrt{C_5} h_2}{\sqrt{C_4}} \right) \\ \sinh \left(\frac{\sqrt{C_5} h_2}{\sqrt{C_4}} \right) \end{pmatrix} \right) \\ \left(\cosh \left(\frac{\sqrt{C_5} h_2}{\sqrt{C_4}} \right) - \sinh \left(\frac{\sqrt{C_5} h_2}{\sqrt{C_4}} \right) \right) C_4^{3/2} \begin{pmatrix} C_7 - \cosh \left(\frac{2\sqrt{C_5} h_2}{\sqrt{C_4}} \right) C_8 \\ \sinh \left(\frac{2\sqrt{C_5} h_2}{\sqrt{C_4}} \right) C_8 \end{pmatrix} \\ + \frac{1}{2} E R_m h_2^2 - \frac{1}{2} R_m C_{10} h_2^2 \end{array} \right\}, \quad (2.54)$$

$$C_{23} = \left\{ \begin{array}{l} \left(\frac{R_m \sin \sqrt{C_1} h_2 C_2 C_6}{C_1 (C_1 C_4 + C_5)} + \frac{R_m \cos \sqrt{C_1} h_2 C_3 C_6}{C_1 (C_1 C_4 + C_5)} + \frac{1}{C_5^{3/2}} R_m \begin{pmatrix} \cosh \left(\frac{\sqrt{C_5} h_2}{\sqrt{C_4}} \right) \\ \sinh \left(\frac{\sqrt{C_5} h_2}{\sqrt{C_4}} \right) \end{pmatrix} \right) \\ C_4^{3/2} \left(C_7 - \cosh \left(\frac{2\sqrt{C_5} h_2}{\sqrt{C_4}} \right) C_8 - \sinh \left(\frac{2\sqrt{C_5} h_2}{\sqrt{C_4}} \right) C_8 \right) + \\ \frac{1}{2} E R_m h_2^2 - \frac{1}{2} R_m C_{10} h_2^2 \end{array} \right\}, \quad (2.55)$$

2.3 Results and discussion

In this section, the effects of different physical parameters, nano particle volume friction ϕ , Stommer's number S_1 , magnetic Reynolds R_m and Grashof number Gr on pressure rise and pressure gradient, nanoparticle volume friction ϕ and heat generation Q_0 on the temperature, magnetic Reynolds R_m and Stommer's number S_1 on axial induced magnetic field h_x and current density j_z , nanoparticle volume friction ϕ , Stommer's number S_1 , magnetic Reynolds R_m , Grashof number Gr and heat generation Q_0 on the velocity profiles for both copper nanofluid and water fluid with the help of graphical results are displayed in Figs. (2.1) – (2.6). The expression for the pressure rise is calculated numerically using mathematics software. The trapping bolus phenomenon observing the flow behavior is also manipulated as well with the help of streamlines graphs in the Figs. (2.7) – (2.9).

Fig. 1(a) represents the effects of volume fraction ϕ on the pressure rise Δp . It is noticed here that pressure rise is an increasing function with the increases of ϕ throughout in the retrograde pumping region ($\Delta p > 0, Q < 0$) and peristaltic pumping region ($\Delta p > 0, Q > 0$), while decreasing at the region ($\Delta p < 0, Q < 0$). In Figs. 2.1(b) and 2.1(c). It is measured that Δp gets decreased with the increasing effects of S_1 and R_m for both copper water and pure water cases in the region ($\Delta p > 0, Q > 0$), Where's the Δp increases in the region ($\Delta p < 0, Q < 0$). Fig. 2.1(d) Depicts pressure rise decreases when the values of Gr are increased.

From Fig. 2.2(a) one can see that pressure gradient $\frac{dp}{dx}$ decreases as nanoparticle volume friction is increased. The variation of the S_1 and R_m gives the same behavior on pressure gradient graph, the both show increasing trend as parameters value increases see Figs. 2.2(b) and 2.2(c) for both the cases, copper – water and pure water. The difference between copper Nanofluid and pure water fluid is that the copper Nanofluid contains more pressure than the pure water. We can see the impact of parameters local temperature Grashof number Gr on the variation of pressure gradient $\frac{dp}{dx}$ from Fig. 2.2(d) when all other parameters are kept fixed. It is noted that

pressure gradient decreases as Gr increases. In order to see the difference between copper nanofluid and pure water, we have constructed the table 2.6 grashouf number Gr , and other flow parameters are fixed as $Q = -2.0$, $Q_0 = 0.3$, $Re = 1.0$, $R_m = 1.0$, $\omega = \pi/6$, $a = 0.2$, $b = 0.4$, $d = 1.0$. From table 2.6 we observe that the copper water and pure water, both give us decreasing values of pressure gradient as we increase the value of Gr . Fig. 2.3(a) presents the effects of temperature θ for the different values of volume fraction ϕ one can see that as we increase the ϕ , temperature also increases, we presented the Fig. 2.3(b) to show the behavior of temperature profile with the effect of heat generation parameter Q_0 the temperature θ increases with an increase of Q_0 for both copper – water and pure water cases. The difference between these can be seen from the table 2.3.

Figs. 2.4(a) and 2.4(b) show the variations of magnetic Reynolds and Stommer's number on an axial induced magnetic field h_x versus y . It is interesting to note that in the half region of the channel, the induced magnetic field is in one direction. However, it is in the opposite direction in the other half region of the channel. The Fig. 2.4(a) displays that the magnitude of h_x increases when R_m increases from wall h_1 to the middle of channel, but the decreasing trend is noticed in the other half of the channel keeping R_m increased. On the other hand, the effects of S_1 on h_x are quite opposite in comparison to R_m . We have also presented tables 2.4 and 2.5, to show this difference in copper nanofluid and pure water.

In Figs. 2.5(a) and 2.5(b) the current density j_z is shown as a function of y for Three different values of R_m and S_1 , both of these figures are of parabolic type, In the both figures the magnitude of j_z decreases as the values of R_m and S_1 increase.

It is observed from Fig. 2.6(a) that velocity profile decreases near to both walls of channel but increases in the center of the channel with increase in the value of ϕ . To see the behavior of velocity profile u for the cases of copper water and pure water with the variation of R_m and S_1 , we displayed the Figs. 2.6(b) and 2.6(c). Velocity profile u increases near the walls of channels but in the middle of the channel velocity decreases by increase in R_m and S_1 respectively. We presented the Fig. 2.6(d) to obtain the variation of velocity profile u for varying the magnitude of parameters

Gr . The Fig. depicts that there are two phases i.e., From left wall to center and from center to right wall. In both the cases of pure water and copper nanofluid, velocity profile increases from the left wall of channel to the center of channel on increase of Gr . But opposite behavior is seen from center of the channel to the right wall. Analyzing this difference between copper water and pure water numerically, we have drawn a table. 2.6.

Fig. 2.6(e) discusses the behaviors of Q_0 on u versus y for both, copper water and pure water. One can see that velocity profile does not change to great extent as compare to copper water fluid. We see that velocity is increasing by increase in Q_0 .

A very interesting phenomenon in the fluid transport is trapping. In the wave frame, streamlines under certain circumstances swell to trap a bolus which travels as an inlet with the wave speed. The occurring of an internally circulating bolus stiffened by closed streamline is called trapping. The bolus described as a volume of fluid bounded by a closed streamlines in the wave frame is moved at the wave pattern. Fig. (2.7) shows the streamlines for the various values of the parameter ϕ . It is noted that bolus becomes large when we give greater values to the ϕ . Fig. (2.8) is drawn for the nano copper fluid we see that bolus becomes small when we give greater values of Gr where one can noticed that from Fig. (2.9) in the case of pure water number of trapping bolus is decreasing with increasing as well as size of bolus also decreases.

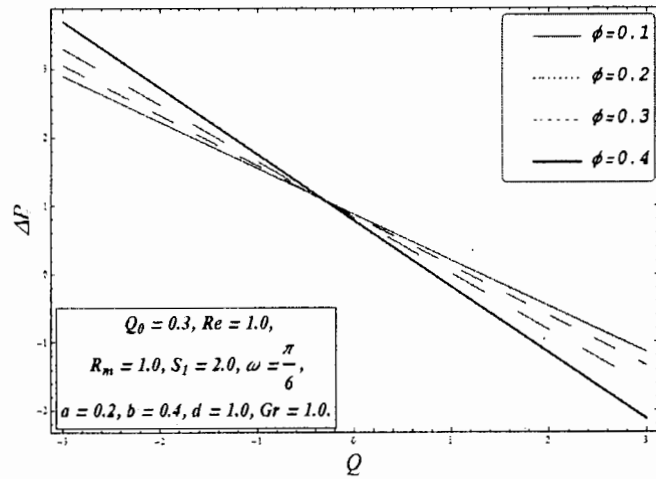


Fig. 2.1 (a): Variation of pressure rise Δp for different value of ϕ .

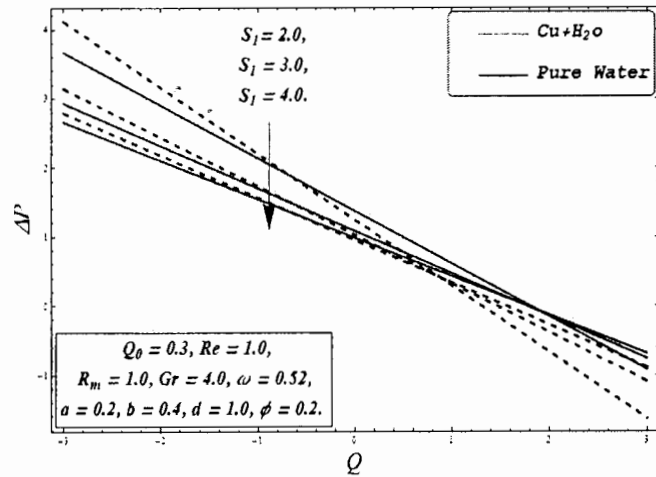


Fig. 2.1 (b): Variation of pressure rise Δp for different values of S_1 .

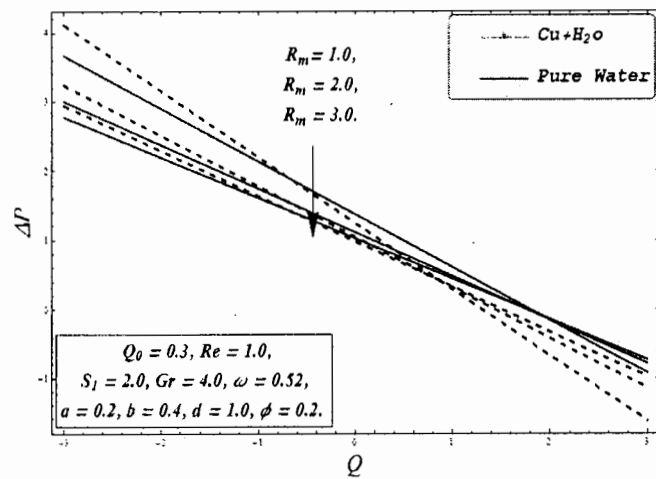
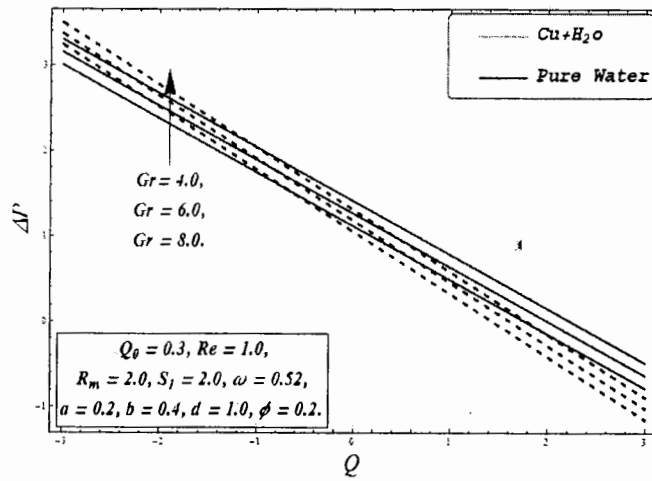


Fig. 2.1 (c): Variation of pressure rise Δp for different values of R_m .



Figs. 2.1 (d): Variation of pressure rise Δp for different values of Gr .

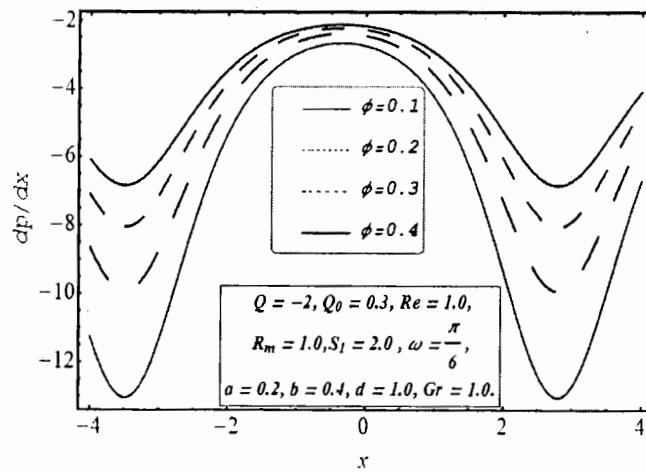


Fig. 2.2 (a): Variation of pressure gradient dp/dx for different values of ϕ .

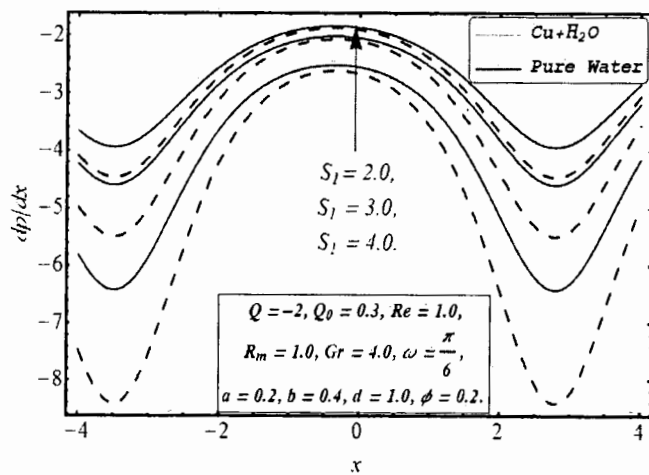


Fig. 2.2 (b): Variation of pressure gradient dp/dx for different values of S_1 .

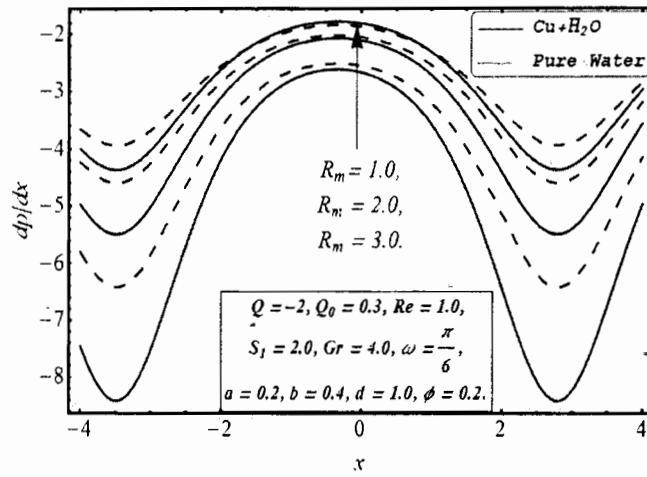


Fig. 2.2 (c): Variation of pressure gradient dp/dx for different values of R_m .

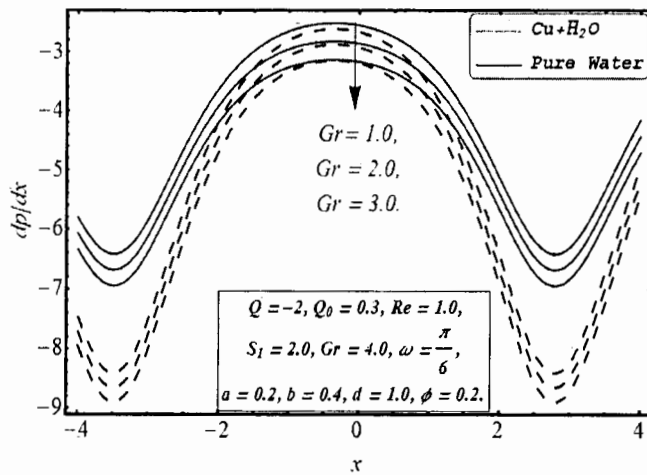


Fig. 2.2 (d): Variation of pressure gradient dp/dx for different values of Gr .

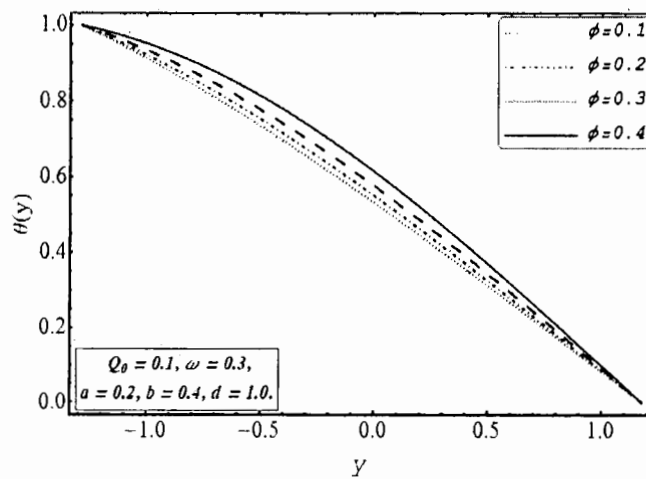


Fig. 2.3 (a): Variation of temperature profile θ for different values of ϕ .

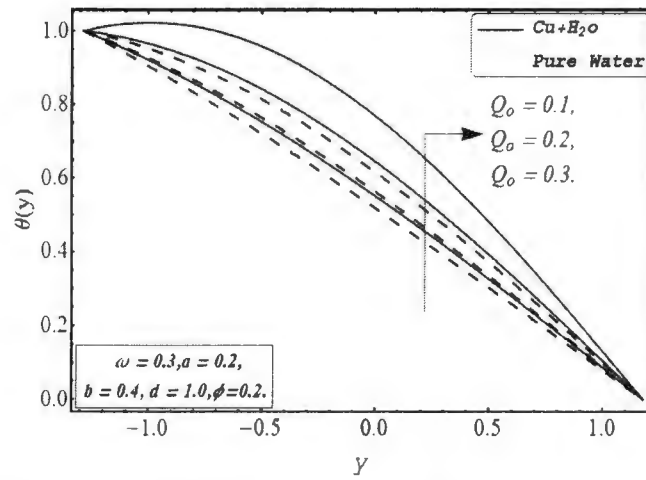


Fig. 2.3 (b): Variation of temperature profile θ for different values of Q_0 .

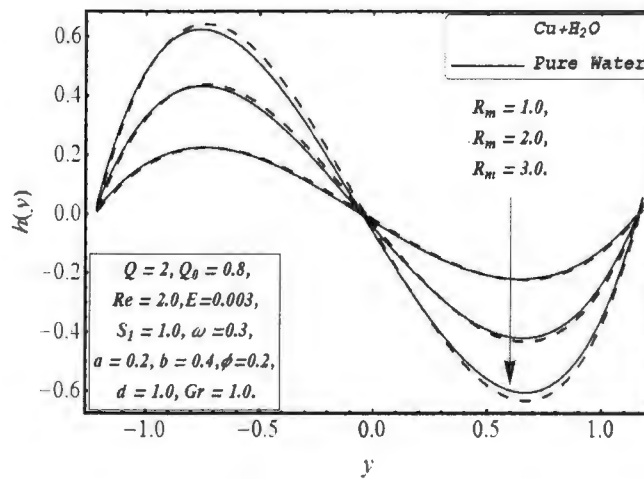


Fig. 2.4(a): Variation of axial induced magnetic field h_x for different values of R_m .

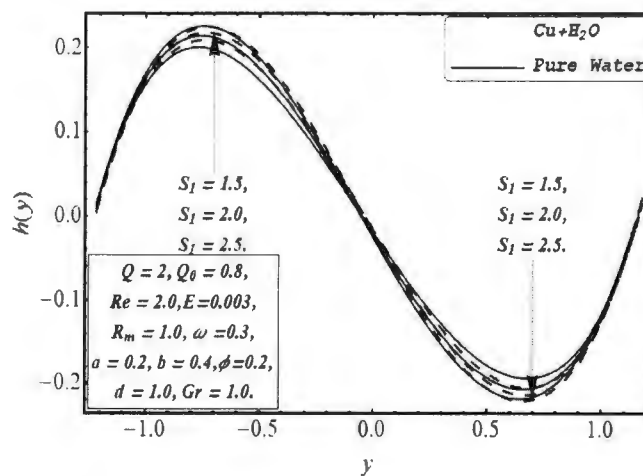


Fig. 2.4(b): Variation of axial induced magnetic field h_x for different values of S_1 .

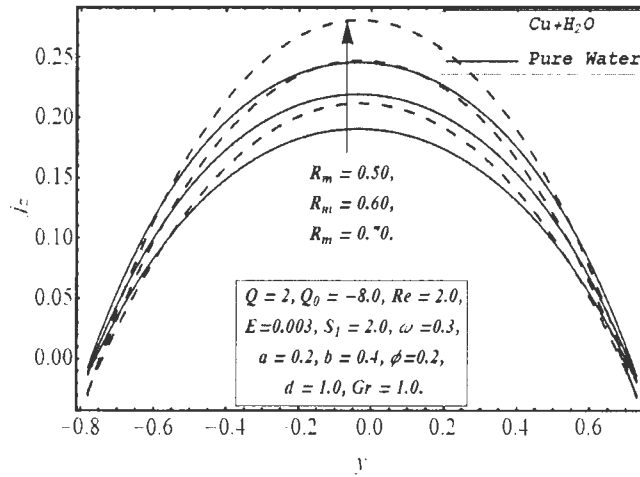


Fig. 2.5(a): Variation of current density j_z for different values of R_m .

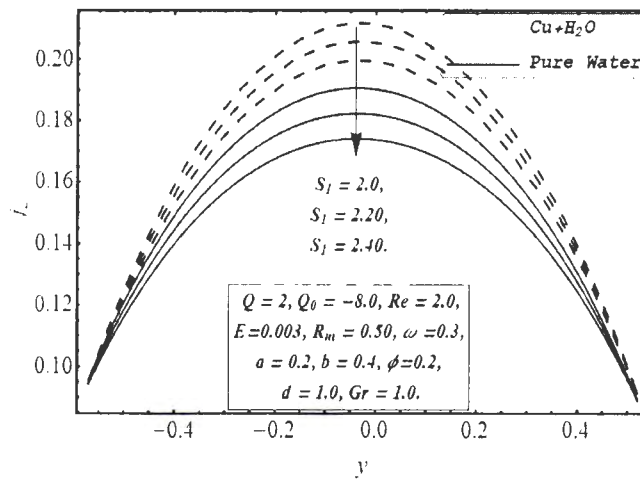


Fig. 2.5(b): Variation of current density j_z for different values of S_1 .

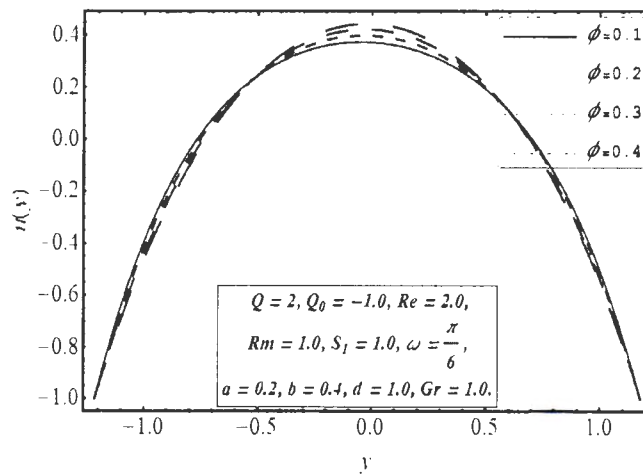


Fig. 2.6 (a): Variation of velocity profile $u(y)$ for different values of ϕ .

TH-16775

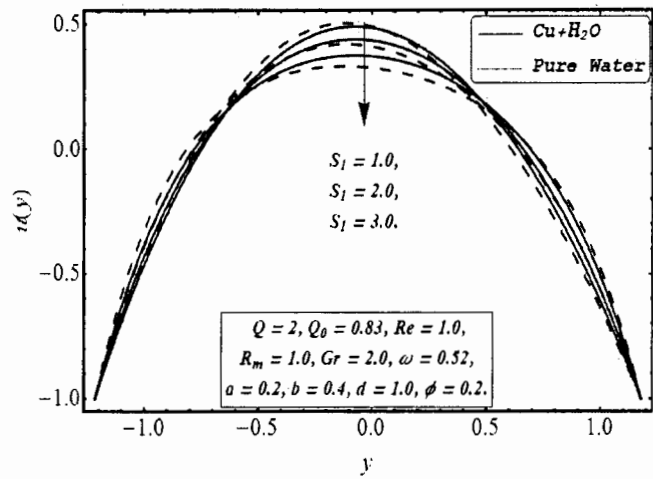


Fig. 2.6 (b): Variation of velocity profile $u(y)$ for different values of S_1 .

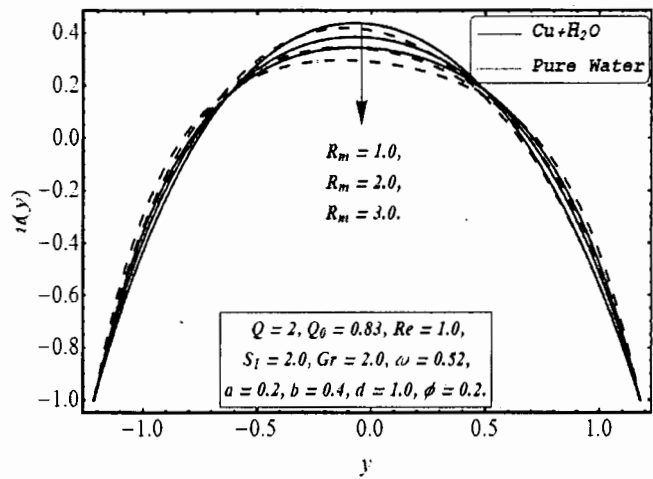


Fig. 2.6 (c): Variation of velocity profile $u(y)$ for different values of R_m .

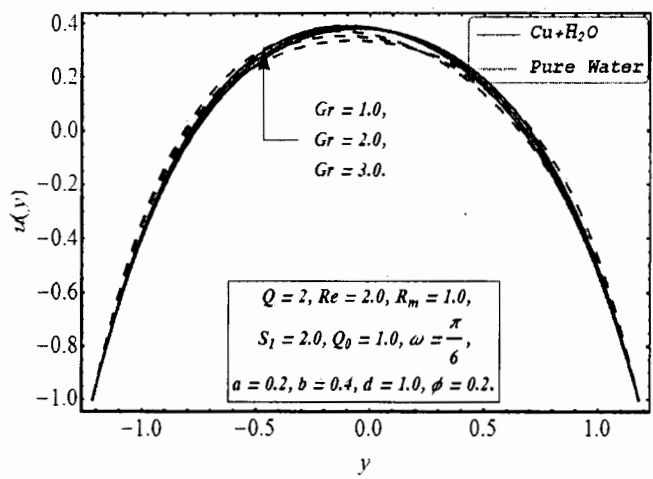


Fig. 2.6 (d): Variation of velocity profile $u(y)$ different value of Gr .

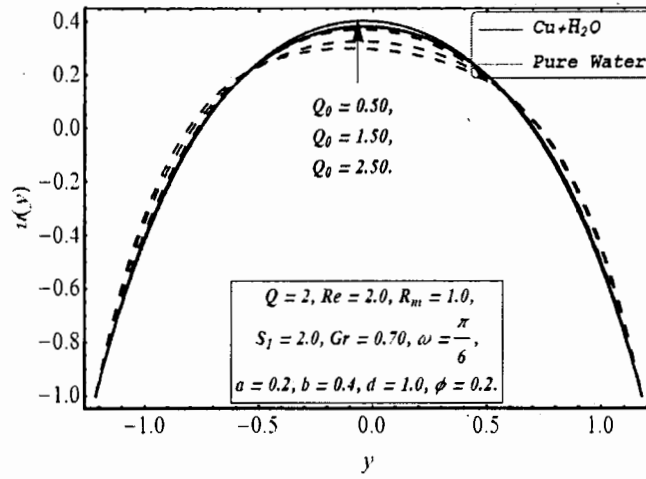
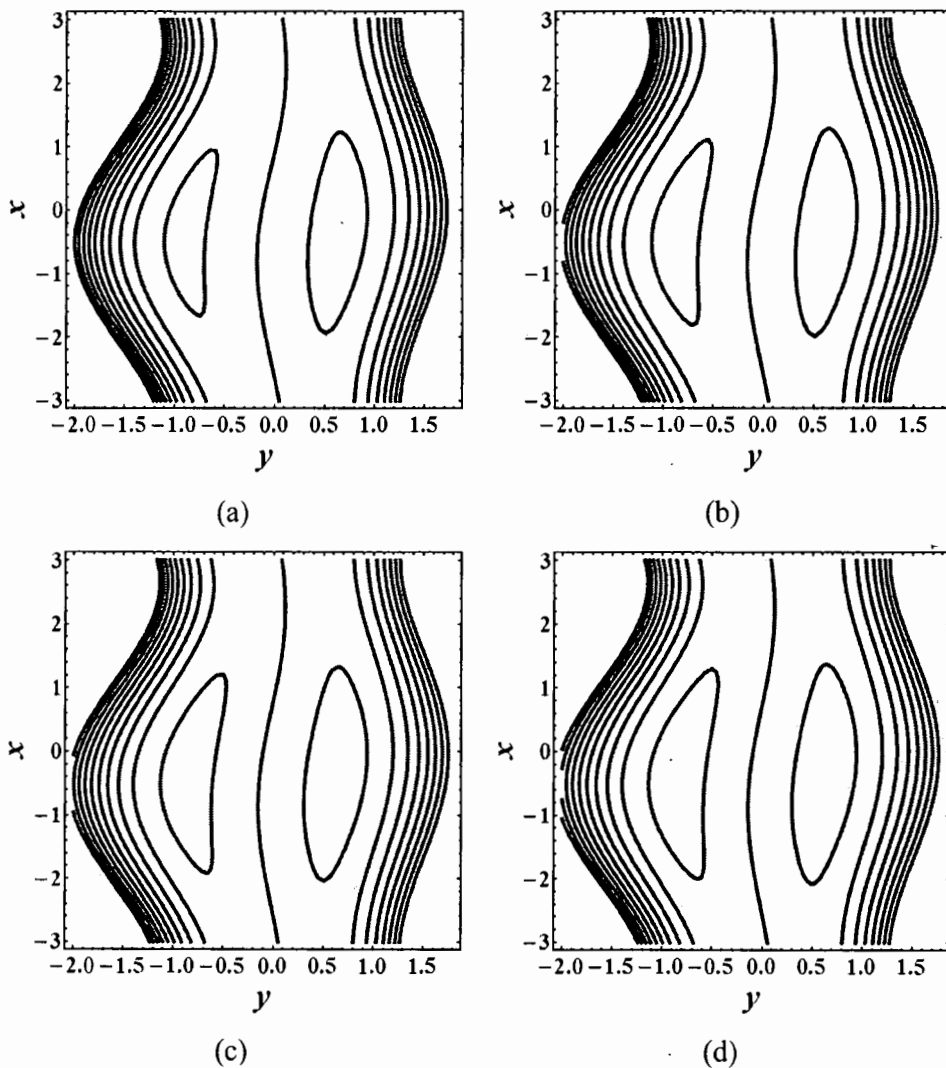
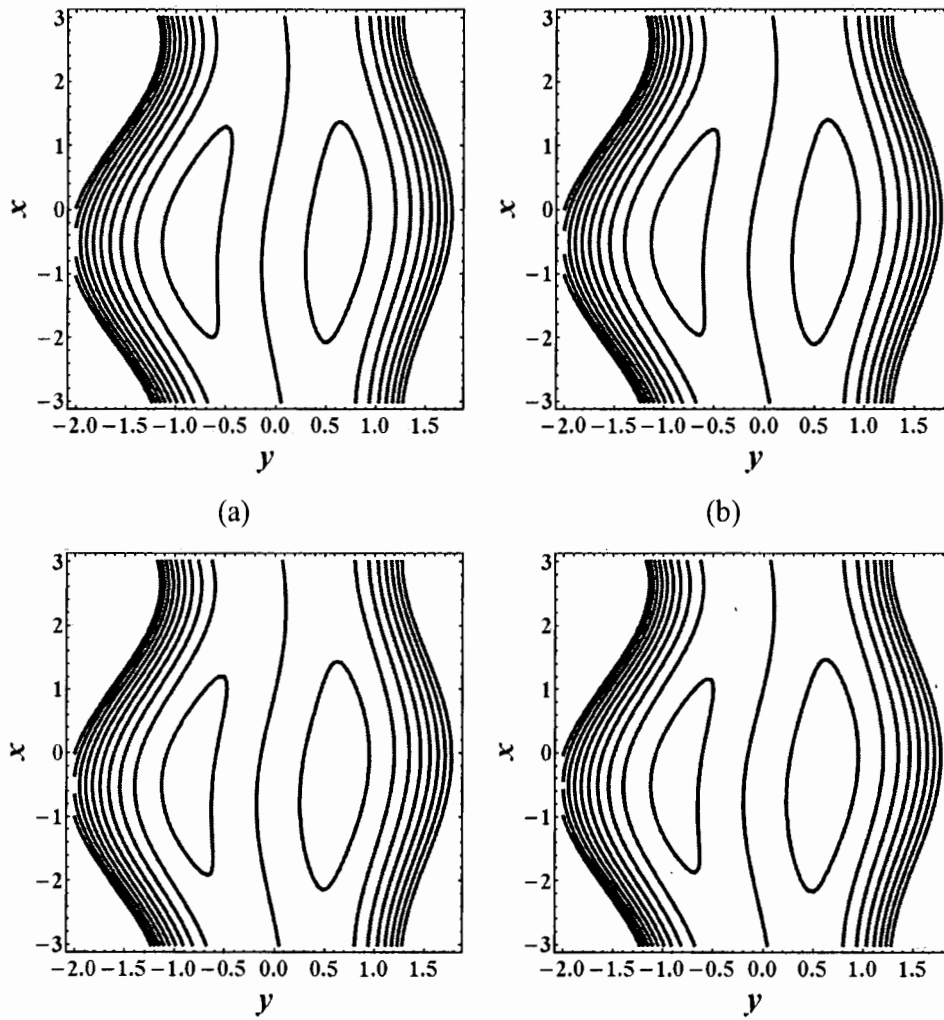


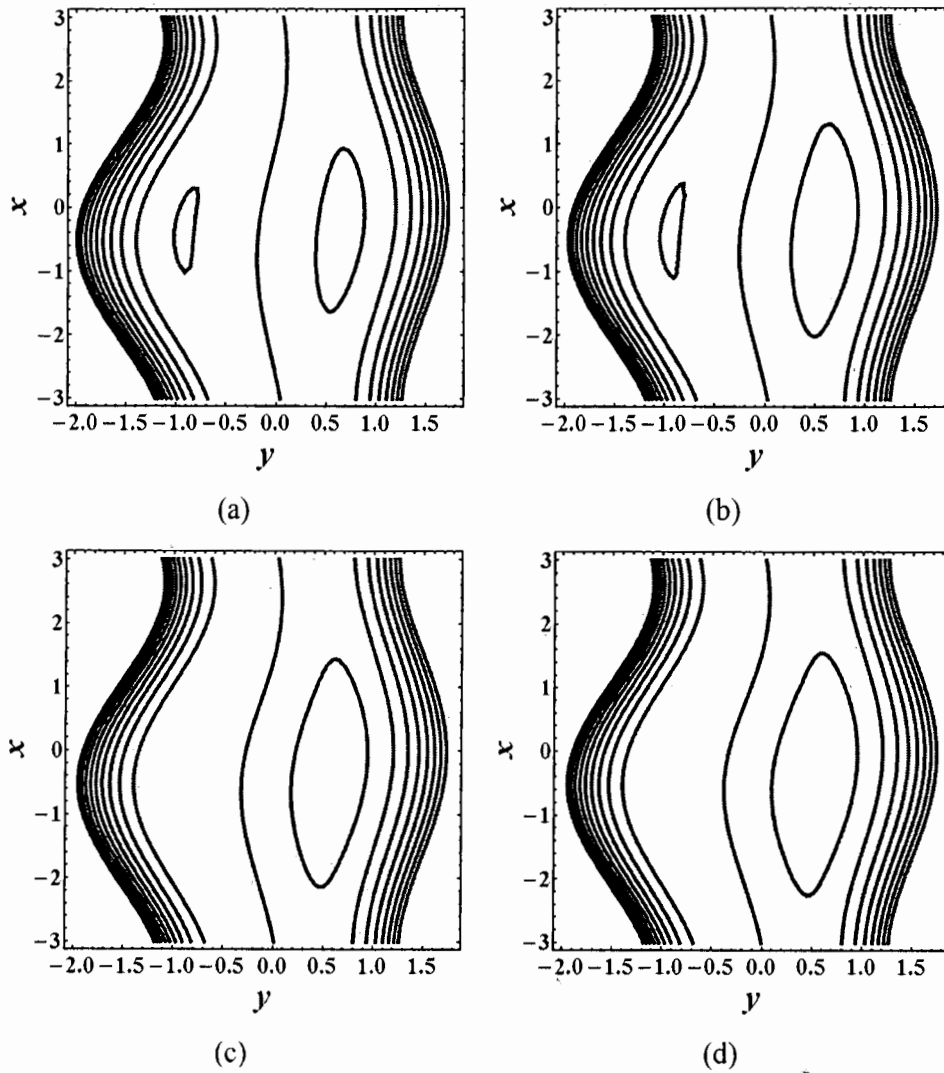
Fig.2.6 (e): Variation of velocity profile $u(y)$ for different values of Q_0 .



Figs.2.7: Stream lines for different values of ϕ . (a) for $\phi=0.1$, (b) for $\phi=0.2$, (c) for $\phi=0.3$, (d) for $\phi=0.4$. The other parameters are $Q=2$, $\omega=0.3$, $a=0.2$, $b=0.4$, $d=1.0$, $Gr=1.0$, $R_m=1.0$, $S_1=2$, $Re=1.0$, $Q_0=0.1$.



Figs. 2.8: Stream lines of copper water nanofluid for different values of Gr .(a) for $Gr=1$, (b) for $Gr=2$, (c) for $Gr=3$, (d) for $Gr=4$. The other parameters are $Q=2$, $\omega=0.3$, $a=0.2$, $b=0.4$, $d=1.0$, $\phi=0.4$, $R_m=1.0$, $S_1=2$, $Re=1.0$, $Q_0=0.1$.



Figs. 2.9: Stream lines of water for different values of Gr . (a) for $Gr=1$, (b) for $Gr=2$, (c) for $Gr=3$, (d) for $Gr=4$. The other parameters are $Q=2$, $\omega=0.3$, $a=0.2$, $b=0.4$, $d=1.0$, $\phi=0.4$, $R_m=1.0$, $S_1=2$, $Re=1.0$, $Q_0=0.1$.

Table 2.2. Numerical values of pressure gradient for different values of Gr .

x	$Gr = 4.0$		$Gr = 6.0$		$Gr = 8.0$	
	$Cu + H_2O$	H_2O	$Cu + H_2O$	H_2O	$Cu + H_2O$	H_2O
	$\phi = 0.2$	$\phi = 0.0$	$\phi = 0.2$	$\phi = 0.0$	$\phi = 0.2$	$\phi = 0.0$
	dp/dx	dp/dx	dp/dx	dp/dx	dp/dx	dp/dx
-4.0	-7.45898	-5.80246	-7.70392	-6.07018	-7.94885	-6.3379
-3.5	-8.40545	-6.41301	-8.64947	-6.67893	-8.89348	-6.94485
-3.0	-7.50832	-5.83445	-7.75321	-6.10206	-7.99809	-6.36967
-2.5	-5.69033	-4.64144	-5.93791	-4.91437	-6.18549	-5.1873
-2.0	-4.18391	-3.62207	-4.43594	-3.90397	-4.69797	-4.18587
-1.5	-3.27188	-2.98444	-3.52945	-3.27786	-3.78702	-3.57129
-1.0	-2.80167	-2.64863	-3.06437	-2.95313	-3.32707	-3.25763
-0.5	-2.62158	-2.51917	-2.88708	-2.82991	-3.15259	-3.14064
0.0	-2.66549	-2.55075	-2.93025	-2.85982	-3.19501	-3.16889
0.5	-2.94979	-2.75486	-3.2106	-3.05522	-3.4714	-3.35558
1.0	-3.57585	-3.199	-3.83113	-3.48761	-4.08641	-3.77623
1.5	-4.71482	-3.98793	-4.96847	-4.2658	-5.21853	-4.54367
2.0	-6.43487	-5.13394	-6.68114	-5.40427	-6.92741	-5.6746
2.5	-8.06947	-6.19698	-8.31379	-6.46349	-8.55811	-6.7299
3.0	-8.22803	-6.29902	-8.4722	-6.56525	-8.71638	-6.83147
3.5	-6.74026	-5.33427	-6.98609	-5.60373	-7.23191	-5.87319
4.0	-4.96341	-4.15397	-5.21273	-4.43036	-5.46204	-4.70676

Table 2.3. Numerical values of temperature for different values of Q_0 .

y	$Q_0 = 0.1$		$Q_0 = 0.2$		$Q_0 = 0.3$	
	$Cu + H_2O$	H_2O	$Cu + H_2O$	H_2O	$Cu + H_2O$	H_2O
	$\phi = 0.2$	$\phi = 0.0$	$\phi = 0.2$	$\phi = 0.0$	$\phi = 0.2$	$\phi = 0.0$
	θ	θ	θ	θ	θ	θ
-1.21	1.0000	1.0000	1.0000	1.0000	1.0000	1.0000
-0.81	0.84520	0.85652	0.86049	0.88504	0.87671	0.91688
-0.41	0.68448	0.70100	0.70682	0.74305	0.73070	0.79064
-0.01	0.51750	0.53428	0.54021	0.57734	0.56464	0.62661
0.38	0.35011	0.36349	0.36822	0.39799	0.38779	0.43776
0.78	0.17528	0.18260	0.1852	0.20155	0.19594	0.22348

Table 2.4. Numerical values of axial induced magnetic field for different values of R_m .

y	$R_m = 1$		$R_m = 2$		$R_m = 3$	
	$Cu + H_2O$	H_2O	$Cu + H_2O$	H_2O	$Cu + H_2O$	H_2O
	$\phi = 0.2$	$\phi = 0.0$	$\phi = 0.2$	$\phi = 0.0$	$\phi = 0.2$	$\phi = 0.0$
	h_x	h_x	h_x	h_x	h_x	h_x
-1.21	0.01077	0.01810	0.01932	0.03039	0.02637	0.03952
-0.91	0.19516	0.19675	0.37669	0.37045	0.54693	0.52735
-0.61	0.20900	0.20301	0.39563	0.37163	0.56400	0.51546
-0.31	0.12087	0.11206	0.22651	0.20264	0.31980	0.27768
-0.01	-0.01226	-0.01842	-0.02182	-0.03045	-0.02953	-0.03897
0.28	-0.13606	-0.13664	-0.25347	-0.24323	-0.35620	-0.32962
0.58	-0.21122	-0.20625	-0.40002	-0.37786	-0.57051	-0.52444
0.88	-0.18082	-0.17330	-0.35144	-0.33208	-0.51312	-0.47874

Table 2.5. Numerical values of axial induced magnetic field for different values of S_1 .

y	$S_1 = 1.5$		$S_1 = 2.0$		$S_1 = 2.5$	
	$Cu + H_2O$	H_2O	$Cu + H_2O$	H_2O	$Cu + H_2O$	H_2O
	$\phi = 0.2$	$\phi = 0.0$	$\phi = 0.2$	$\phi = 0.0$	$\phi = 0.2$	$\phi = 0.0$
	h_x	h_x	h_x	h_x	h_x	h_x
-1.21	0.0000	0.0000	0.0000	0.0000	0.0000	0.0000
-0.91	0.18677	0.1827	0.17690	0.16781	0.16650	0.15352
-0.61	0.19524	0.18205	0.17930	0.16017	0.16293	0.13991
-0.31	0.11151	0.09896	0.10073	0.08531	0.08983	0.07290
-0.01	-0.01062	-0.01459	-0.00897	-0.01133	-0.00170	-0.00883
0.28	-0.12462	-0.11842	-0.11178	-0.10042	-0.09904	-0.08469
0.58	-0.19743	-0.18514	-0.18144	-0.16306	-0.16500	-0.14257
0.88	-0.17451	-0.16435	-0.16673	-0.15381	-0.15819	-0.14286

Table 2.6. Numerical values of velocity for different values of Gr .

y	$Gr = 1.0$		$Gr = 2.0$		$Gr = 3.0$	
	$Cu + H_2O$	H_2O	$Cu + H_2O$	H_2O	$Cu + H_2O$	H_2O
	$\phi = 0.2$	$\phi = 0.0$	$\phi = 0.2$	$\phi = 0.0$	$\phi = 0.2$	$\phi = 0.0$
	u	u	u	u	u	u
-1.21	-1.0000	-1.0000	-1.0000	-1.0000	-1.0000	-1.0000
-0.91	-0.2201	-0.1717	-0.2072	-0.1598	-0.1944	-0.1479
-0.61	0.1655	0.1751	0.1813	0.1970	0.1972	0.2189
-0.31	0.3398	0.3105	0.3516	0.3335	0.3633	0.3565
-0.01	0.3811	0.3351	0.3840	0.3482	0.3869	0.3613
0.28	0.3177	0.2807	0.3100	0.2758	0.3023	0.2710
0.58	0.1262	0.1222	0.1093	0.0965	0.0924	0.0708
0.88	-0.2642	-0.2305	-0.2821	-0.2647	-0.3001	-0.2989

Table 2.7. Numerical values of velocity for different values of Q_0 .

y	$Q_0 = 0.5$		$Q_0 = 1.5$		$Q_0 = 2.5$	
	$Cu + H_2O$	H_2O	$Cu + H_2O$	H_2O	$Cu + H_2O$	H_2O
	$\phi = 0.2$	$\phi = 0.0$	$\phi = 0.2$	$\phi = 0.0$	$\phi = 0.2$	$\phi = 0.0$
	u	u	u	u	u	u
-1.21	-1.0000	-1.0000	-1.0000	-1.0000	-1.0000	-1.0000
-0.91	-0.2232	-0.1707	-0.2254	-0.2054	0.2392	-0.1427
-0.61	0.1604	0.1680	0.1610	0.1652	0.1595	0.1791
-0.31	0.3350	0.2981	0.3382	0.3307	0.3518	0.2842
-0.01	0.3789	0.3244	0.3826	0.3693	0.4015	0.2967
0.28	0.3194	0.2786	0.3211	0.3066	0.3326	0.2553
0.38	0.2735	0.2439	0.2741	0.2606	0.2808	0.2261
0.88	-0.2573	-0.2136	-0.2612	-0.2531	-0.2775	-0.1964

2.4 Conclusion

Interaction of nanoparticles for the peristaltic flow with the induced magnetic field is discussed, key points are observed as follows:

- i. It is noticed here that pressure rise is an increasing function with the increases of volume fraction throughout in the retrograde pumping region.
- ii. It is measured that pressure rise gets decreased with the increasing effects of stommel's number and magnetic Reynolds, for both copper water and pure water.
- iii. The variation of the magnetic Reynolds gives the same behavior on pressure gradient for both copper water and pure water.
- iv. It is noted that pressure gradient is decreases as increases of Grashof number.
- v. For the different values of volume fraction ϕ , one can see that temperature is an increasing function of volume fraction ϕ .
- vi. Temperature profile increases as the increases of heat generation for both copper water and pure water cases.
- vii. It is observed that for both copper water and pure water cases, velocity profile increases from the left wall of channel to the center of channel on increase of

- Grashof number. But opposite behavior is seen from center of the channel to the right wall.
- viii. It is noted that bolus becomes large when we give greater values of the volume fraction
 - ix. Bolus becomes small with give greater values of Grashof number.

Chapter 3

Nanofluid containing Cu – H₂O treated through Maxwell model with induced magnetic Field in peristaltic

The objective of this chapter is to study nanofluid containing copper (Cu) particle with different shapes in viscous fluids for the peristaltic flow. The base fluid is water and nanoparticles are of copper having shapes bricks, cylindrical and platelets. The flow will be considered over the two dimensional wavy channel. The momentum and continuity equation with the interaction of nanofluid under induced magnetic field are used to model the governing equations. This leads to coupled boundary value problem. The influence of nanoparticle volumetric friction, shape factor, magnetic Reynold's number, Stommer's number and other physical parameters will be highlighted through graphs.

3.1 Mathematical formulation

After using the relation Eq. (2.9) and non – dimensional parameters Eq. (2.10), the governing Eqs. (2.2), (2.3) and (2.4) (without using bar) for nanofluid take the following form:

$$\frac{\partial u}{\partial x} + \frac{\partial v}{\partial y} = 0, \quad (3.1)$$

$$\frac{dp}{dx} = \frac{\partial^3 \psi}{\partial y^3} \left(\frac{1}{(1-\phi)^{2.5}} \right) + \text{Re} S_1^2 \Phi_{,yy} + \frac{(\rho\beta)_{nf}}{(\rho\beta)_f} Gr\theta, \quad (3.2)$$

$$\frac{dp}{dy} = 0, \quad (3.3)$$

$$\Phi_{,yy} = R_m \left(E - \frac{\partial \psi}{\partial y} \right), \quad (3.4)$$

$$\frac{\partial^2 \theta}{\partial y^2} + \theta \frac{k_f}{k_{nf}} Q_0 = 0. \quad (3.5)$$

Putting Eq. (3.14) into Eq. (3.12), we get

$$\frac{dp}{dx} = \frac{\partial^3 \psi}{\partial y^3} \left(\frac{1}{(1-\phi)^{2.5}} \right) + \text{Re} S_1^2 R_m \left(E - \frac{\partial \psi}{\partial y} \right) + \frac{(\rho\beta)_{nf}}{(\rho\beta)_f} Gr \theta. \quad (3.6)$$

Taking derivative of above equation with respect to y we have

$$\frac{\partial^4 \psi}{\partial y^4} \left(\frac{1}{(1-\phi)^{2.5}} \right) + \text{Re} S_1^2 R_m \left(-\frac{\partial^2 \psi}{\partial y^2} \right) + \frac{(\rho\beta)_{nf}}{(\rho\beta)_f} Gr \frac{\partial \theta}{\partial y} = 0. \quad (3.7)$$

The non-dimensional boundaries will take the form as

$$\psi = \frac{F}{2}, \quad \frac{\partial \psi}{\partial y} = -1, \quad \text{at} \quad y = h_1, \quad (3.8)$$

$$\psi = -\frac{F}{2}, \quad \frac{\partial \psi}{\partial y} = -1, \quad \text{at} \quad y = h_2, \quad (3.9)$$

$$\theta = 0 \quad \text{at} \quad y = h_1, \quad \theta = 1 \quad \text{at} \quad y = h_2, \quad (3.10)$$

$$\Phi = 0 \quad \text{at} \quad y = h_1, \quad \Phi = 0 \quad \text{at} \quad y = h_2. \quad (3.11)$$

The pressure rise Δp , axial induced magnetic h_x and current density j_z in non-dimensional form is defined as




$$\Delta p = \int_0^1 \frac{dp}{dx} dx, \quad (3.12)$$

$$h_x = \frac{\partial \Phi}{\partial y}, \quad (3.13)$$

$$j_z = \frac{\partial h_x}{\partial y}. \quad (3.14)$$

$$k_{nf} = k_f \left(\frac{k_s + (1+m)k_f - (1+m)\phi(k_f - k_s)}{k_s + (1+m)k_f + \phi(k_f - k_s)} \right). \quad (3.15)$$

Where k_s and k_f are the conductivities of the particle material and the base fluid. In this Hamilton – Crosser model, m is the shape factor. Elena et al. [21] investigated thermal conductivity and viscosity of various shapes of Copper nanoparticles in a fluid. They analyzed experimental data accompanied by theoretical modeling for different shapes of nanoparticles. According to them, the values of shape factor are given as in the table 3.1.

Nanoparticle name	Shapes	Shape factor
Bricks		3.7
Cylinder		4.9
Platelets		5.7

3.2 Solution of the problem

Exact solutions of Eqs. (3.4), (3.5) and (3.7) subject to boundary conditions (3.8 – 3.11) are found as follows:

$$\theta(y) = \csc \left(Q_0 \sqrt{\frac{k_f}{k_{nf}}} (h_1 - h_2) \right) \sin \left(Q_0 \sqrt{\frac{k_f}{k_{nf}}} (h_1 - y) \right), \quad (3.16)$$

where

$$\psi(y) = \left. \begin{aligned} &C_{32} + yC_{33} + C_{30}C_{35} \cosh C_{34}y + C_{31}C_{35} \cosh(C_{34}y) \\ &-C_{10}C_{35} \sinh C_{34}y + C_{31}C_{35} \sinh C_{34}y - C_{25}C_{36} \cos y\sqrt{C_{24}} \\ &+ C_{26}C_{36} \sin y\sqrt{C_{24}} \end{aligned} \right\}, \quad (3.17)$$

$$\Phi(y) = C_{45} + yC_{46} + \frac{\left. \begin{aligned} & \sqrt{C_{24}} \left(y^2 (E - C_{33}) C_{34} + \right. \\ & \left. 2 \left(\cosh y C_{34} \right. \right. \\ & \left. \left. \left((C_{10} - C_{31}) - \sinh y C_{34} (C_{30} + C_{31}) \right) C_{35} \right) \right) + \\ & \left. 2 \left(\begin{aligned} & \sin y \sqrt{C_{24}} C_{25} \\ & + \cos y \sqrt{C_{24}} C_{26} \end{aligned} \right) C_{34} C_{36} \right)}{2\sqrt{C_{24}} C_{34}} R_m \quad (3.18) \end{aligned}$$

The mean volume flow rate Q over one period is given as

$$Q = F + 1 + d, \quad (3.19)$$

and pressure gradient dp/dx axial induced magnetic h_x and current density j_z are elaborated as

$$\begin{aligned}
& -1 + \cosh C_{34} h_1 C_{10} C_{34} C_{35} - \sin \sqrt{C_{24}} h_1 \sqrt{C_{24}} C_{25} C_{36} - \cos \sqrt{C_{24}} h_1 \sqrt{C_{24}} C_{26} C_{36} + \\
& \left(\begin{aligned} & (\cosh C_{34} h_1 C_{34} C_{35} + \sinh C_{34} h_1 C_{34} C_{35}) \\ & \left(\begin{aligned} & -\cosh C_{34} h_1 C_{10} C_{34} C_{35} + \cosh C_{34} h_2 C_{10} C_{34} C_{35} + \sin \sqrt{C_{24}} h_1 \sqrt{C_{24}} C_{25} C_{36} \\ & -\sin \sqrt{C_{24}} h_2 \sqrt{C_{24}} C_{25} C_{36} + \cos \sqrt{C_{24}} h_1 \sqrt{C_{24}} C_{26} C_{36} - \cos \sqrt{C_{24}} h_2 \\ & \sqrt{C_{24}} C_{26} C_{36} \end{aligned} \right) \end{aligned} \right) \\
\frac{dp}{dx} = & \frac{\left(\begin{aligned} & (\cosh C_{34} h_1 - \cosh C_{34} h_2 + \sinh C_{34} h_1 - \sinh C_{34} h_2) \\ & C_{34} C_{35} \end{aligned} \right)}{\left(\begin{aligned} & (-\cosh C_{34} h_2 \sinh C_{34} h_1 C_{34} C_{35}) \\ & (+\cosh C_{34} h_1 \sinh C_{34} h_2 C_{34} C_{35}) \end{aligned} \right)} \quad (3.20) \\
& + \left(\begin{aligned} & \left(\begin{aligned} & F + \sinh C_{34} h_1 C_{10} C_{35} \\ & -\sinh C_{34} h_2 C_{10} C_{35} + \cos \sqrt{C_{24}} h_1 C_{25} C_{36} \\ & -C_{43} - \cos \sqrt{C_{24}} h_2 \\ & C_{25} C_{36} - \sin \sqrt{C_{24}} h_1 C_{26} C_{36} + \sin \sqrt{C_{24}} h_2 C_{26} C_{36} \\ & - \left(\begin{aligned} & 1 - \cosh C_{34} h_1 C_{10} C_{34} C_{35} \\ & + \sin \sqrt{C_{24}} h_1 \sqrt{C_{24}} C_{25} C_{36} + \cos \sqrt{C_{24}} h_1 \sqrt{C_{24}} C_{26} C_{36} \end{aligned} \right) (-h_1 + h_2) \end{aligned} \right) \end{aligned} \right) \\
& C_{44}
\end{aligned}$$

$$h_\lambda = C_{46} + \frac{1}{2\sqrt{C_{24}} C_{34}} \left(\begin{aligned} & \sqrt{C_{24}} \left(\begin{aligned} & 2y(E - C_{33})C_{34} + \\ & 2 \left(\begin{aligned} & \sinh y C_{34} (C_{10} - C_{31})C_{34} \\ & -\cosh y C_{34} (C_{30} + C_{31})C_{34} \end{aligned} \right) C_{35} \end{aligned} \right) \\ & + 2 \left(\begin{aligned} & \cos y \sqrt{C_{24}} \sqrt{C_{24}} C_{25} - \\ & \sin y \sqrt{C_{24}} \sqrt{C_{24}} C_{26} \end{aligned} \right) C_{34} C_{36} \end{aligned} \right) R_m \quad (3.21)$$

	$j_z = \frac{1}{2\sqrt{C_{24}C_{34}}} \left\{ \begin{array}{l} \sqrt{C_{24}} \left(2(E - C_{33})C_{34} + 2 \left(\cosh yC_{34}(C_{10} - C_{31})C_{34}^2 - \right. \right. \\ \left. \left. \sinh yC_{34}(C_{30} + C_{31})C_{34}^2 \right) C_{35} \right) \\ + 2 \left(\begin{array}{l} -\sin y\sqrt{C_{24}C_{24}C_{25}} \\ -\cos y\sqrt{C_{24}C_{24}C_{26}} \end{array} \right) C_{34}C_{36} \end{array} \right\} R_m, \quad (3.22)$	
	<p>the constants $C_{24} - C_{46}$ are obtained by using Mathematica 9.</p> $C_{24} = \frac{k_s + (1+m)k_f + \phi(k_f - k_s)}{k_s + (1+m)k_f - (1+m)(k_f - k_s)\phi} Q_0, \quad (3.23)$	
	$C_{25} = \frac{\cos \sqrt{C_{24}}h_1}{-\cos \sqrt{C_{24}}h_2 \sin \sqrt{C_{24}}h_1 + \cos \sqrt{C_{24}}h_1 \sin \sqrt{C_{24}}h_2}, \quad (3.24)$	
	$C_{26} = \frac{\sin \sqrt{C_{24}}h_1}{\cos \sqrt{C_{24}}h_2 \sin \sqrt{C_{24}}h_1 - \cos \sqrt{C_{24}}h_1 \sin \sqrt{C_{24}}h_2}, \quad (3.25)$	
	$C_{27} = \frac{1}{(1-\phi)^{2.5}}, \quad (3.26)$	
	$C_{28} = \text{Re} S_1^2 R_m, \quad (3.27)$	
	$C_{29} = \frac{(\rho\beta)_{nf}}{(\rho\beta)_f} Gr, \quad (3.28)$	
	$C_{30} = \frac{\left(\begin{array}{l} \cosh C_{34}h_1 C_{10} C_{34} C_{35} - \cosh C_{34}h_2 C_{10} C_{34} C_{35} - \\ \sin \sqrt{C_{24}}h_1 \sqrt{C_{24}}C_{25}C_{36} + \sin \sqrt{C_{24}}h_2 \sqrt{C_{24}}C_{25}C_{36} \\ - \cos \sqrt{C_{24}}h_1 \sqrt{C_{24}}C_{26}C_{36} + \cos \sqrt{C_{24}}h_2 \sqrt{C_{24}}C_{26}C_{36} \end{array} \right) C_{37}}{\left(\begin{array}{l} -\cosh C_{34}h_1 C_{35} + \cosh C_{34}h_2 C_{35} - \sinh C_{34}h_1 C_{35} + \\ C_{38} \sinh C_{34}h_2 C_{35} - (\cosh C_{34}h_1 C_{34} C_{35} + \sinh C_{34}h_1 C_{34} C_{35}) \\ (-h_1 + h_2) \end{array} \right) \right)}, \quad (3.29)$	

$$C_{31} = \left. \begin{aligned} & \left(\frac{-\cosh C_{34} h_1 C_{10} C_{34} C_{35} + \cosh C_{34} h_2 C_{10} C_{34} C_{35} + \sin \sqrt{C_{24}} h_1 \sqrt{C_{24}} C_{25} C_{36} - \sin \sqrt{C_{24}} h_2 \sqrt{C_{24}} C_{25} C_{36} + \cos \sqrt{C_{24}} h_1 \sqrt{C_{24}} C_{26} C_{36} - \cos \sqrt{C_{24}} h_2 \sqrt{C_{24}} C_{26} C_{36}}{\begin{pmatrix} \cosh C_{34} h_1 - \\ \cosh C_{34} h_2 + \\ \sinh C_{34} h_1 - \\ \sinh C_{34} h_2 \end{pmatrix} C_{34} C_{35}} \right) + \\ & \left(\frac{\begin{pmatrix} -\sinh C_{34} h_1 C_{34} C_{35} + \sinh C_{34} h_2 \\ C_{34} C_{35} \end{pmatrix} C_{39}}{\begin{pmatrix} -\cosh C_{34} h_1 C_{34} C_{35} \\ + \cosh C_{34} h_2 C_{34} C_{35} - \sinh C_{34} h_1 C_{34} C_{35} + \sinh C_{34} h_2 C_{34} C_{35} \end{pmatrix} C_{40}} \right) \end{aligned} \right\} \quad (3.30)$$

$$C_{32} = \left. \begin{aligned} & \frac{1}{2} \left(\frac{F + 2 \sinh C_{34} h_1 C_{10} C_{35} + 2 \cos \sqrt{C_{24}} h_1 C_{25} C_{36} - 2 \sin \sqrt{C_{24}} h_1}{C_{26} C_{36}} \right) + \\ & \left(\frac{1 - \cosh C_{34} h_1 C_{10} C_{34} C_{35} + \sin \sqrt{C_{24}} h_1 \sqrt{C_{24}} C_{25} C_{36} + \cos \sqrt{C_{24}} h_1 \sqrt{C_{24}} C_{26} C_{36}}{\begin{pmatrix} -\cosh C_{34} h_1 C_{10} C_{34} C_{35} + \\ \cosh C_{34} h_2 C_{10} C_{34} C_{35} + \sin \sqrt{C_{24}} h_1 \sqrt{C_{24}} C_{25} C_{36} - \\ \sin \sqrt{C_{24}} h_2 \sqrt{C_{24}} C_{25} C_{36} + \cos \sqrt{C_{24}} h_1 \sqrt{C_{24}} C_{26} C_{36} - \\ \cos \sqrt{C_{24}} h_2 \\ \sqrt{C_{24}} C_{26} C_{36} \end{pmatrix}} \right) h_1 + \\ & \left(\frac{\begin{pmatrix} \cosh C_{34} h_1 C_{35} + \sinh C_{34} h_1 C_{35} - \cosh C_{34} h_1 C_{34} C_{35} h_1 - \\ \sinh C_{34} h_1 C_{34} C_{35} h_1 \end{pmatrix}}{\begin{pmatrix} \cosh C_{34} h_1 - \cosh C_{34} h_2 + \sinh C_{34} h_1 - \\ \sinh C_{34} h_2 \end{pmatrix} C_{34} C_{35}} \right) + \\ & \left(\frac{\begin{pmatrix} \cosh (C_{34} h_1)^2 C_{35} - \cosh C_{34} h_1 \cosh C_{34} h_2 C_{35} - \\ \sinh (C_{34} h_1)^2 C_{35} + \sinh C_{34} h_1 \sinh C_{34} h_2 C_{35} + \\ \cosh C_{34} h_2 \sinh C_{34} h_1 \\ C_{34} C_{35} h_1 - \cosh C_{34} h_1 \sinh C_{34} h_2 C_{34} C_{35} h_1 \end{pmatrix} C_{41}}{C_{42}} \right) \end{aligned} \right\} \quad (3.31)$$

$ \begin{aligned} & -1 + \cosh C_{34} h_1 C_{10} C_{34} C_{35} - \sin \sqrt{C_{24}} h_1 \sqrt{C_{24}} C_{25} C_{36} \\ & - \cos \sqrt{C_{24}} h_1 \\ & \left(\begin{aligned} & (\cosh C_{34} h_1 C_{34} C_{35} + \sinh C_{34} h_1 C_{34} C_{35}) \\ & (-\cosh C_{34} h_1 C_{10} C_{34} C_{35} + \cosh C_{34} h_2 C_{10} C_{34} C_{35} + \\ & \sin \sqrt{C_{24}} h_1 \sqrt{C_{24}} C_{25} C_{36} - \sin \sqrt{C_{24}} h_2 \sqrt{C_{24}} C_{25} C_{36} \\ & + \cos \sqrt{C_{24}} h_1 \sqrt{C_{24}} C_{26} C_{36} - \cos \sqrt{C_{24}} h_2 \\ & \sqrt{C_{24}} C_{26} C_{36} \end{aligned} \right) \\ C_{33} = & \frac{\sqrt{C_{24}} C_{26} C_{36} + \left(\begin{aligned} & (\cosh C_{34} h_1 - \cosh C_{34} h_2 + \sinh C_{34} h_1 - \sinh C_{34} h_2) \\ & C_{34} C_{35} \end{aligned} \right)}{\left(\begin{aligned} & (-\cosh C_{34} h_2 \sinh C_{34} h_1 C_{34} C_{35}) \\ & + \cosh C_{34} h_1 \sinh C_{34} h_2 C_{34} C_{35} \\ & \left(\begin{aligned} & F + \sinh C_{34} h_1 C_{10} C_{35} \\ & -\sinh C_{34} h_2 C_{10} C_{35} + \cos \sqrt{C_{24}} h_1 C_{25} C_{36} - \cos \sqrt{C_{24}} h_2 \\ & -C_{43} C_{25} C_{36} - \sin \sqrt{C_{24}} h_1 C_{26} C_{36} + \sin \sqrt{C_{24}} h_2 C_{26} C_{36} - \\ & \left(\begin{aligned} & 1 - \cosh C_{34} h_1 C_{10} C_{34} C_{35} \\ & + \sin \sqrt{C_{24}} h_1 \sqrt{C_{24}} C_{25} C_{36} + \cos \sqrt{C_{24}} h_1 \sqrt{C_{24}} C_{26} C_{36} \end{aligned} \right) (-h_1 + h_2) \end{aligned} \right) \end{aligned} \right)} \\ & C_{44} \end{aligned} $	(3.32)
$C_{34} = \frac{\sqrt{C_{28}}}{\sqrt{C_{27}}},$	(3.33)
$C_{35} = \frac{C_{27}}{C_{28}},$	(3.34)
$C_{36} = \frac{C_{29}}{\sqrt{C_{24}} (C_{24} C_{27} + C_{28})},$	(3.35)

$C_{37} = \left(\begin{array}{l} -\cosh C_{34} h_1 C_{35} + \cosh C_{34} h_2 C_{35} \\ -\sinh C_{34} h_1 C_{35} + \sinh C_{34} h_2 C_{35} - \\ (\cosh C_{34} h_1 C_{34} C_{35} + \sinh C_{34} h_1 C_{34} C_{35}) \\ (-h_1 + h_2) \end{array} \right) +$ $\left(\begin{array}{l} -\cosh C_{34} h_1 C_{34} C_{35} + \cosh C_{34} h_2 C_{34} C_{35} - \\ \sinh C_{34} h_1 C_{34} C_{35} + \sinh C_{34} h_2 C_{34} C_{35} \end{array} \right)$ $\left(\begin{array}{l} F + \sinh C_{34} h_1 C_{10} C_{35} - \sinh C_{34} h_2 C_{10} C_{35} + \cos \sqrt{C_{24}} h_1 C_{25} C_{36} - \\ \cos \sqrt{C_{24}} h_2 C_{25} C_{36} - \sin \sqrt{C_{24}} h_1 C_{26} C_{36} + \\ \sin \sqrt{C_{24}} h_2 C_{26} C_{36} - \\ \left(1 - \cosh C_{34} h_1 C_{10} C_{34} C_{35} \right) \\ + \sin \sqrt{C_{24}} h_1 \sqrt{C_{24}} C_{25} C_{36} \\ + \cos \sqrt{C_{24}} h_1 \sqrt{C_{24}} C_{26} C_{36} \end{array} \right) (-h_1 + h_2)$		(3.36)
$C_{38} = \left(\begin{array}{l} -\cosh C_{34} h_1 C_{34} C_{35} + \cosh C_{34} h_2 C_{34} C_{35} - \sinh C_{34} h_1 C_{34} C_{35} + \\ \sinh C_{34} h_2 C_{34} C_{35} \end{array} \right)$ $\left(\begin{array}{l} -\cosh C_{34} h_1 C_{35} + \cosh C_{34} h_2 C_{35} - \\ \sinh C_{34} h_1 C_{34} C_{35} (-h_1 + h_2) \end{array} \right)$ $-(-\sinh C_{34} h_1 C_{34} C_{35} + \sinh C_{34} h_2 C_{34} C_{35})$		(3.37)

$C_{39} = \left. \begin{aligned} & \left(\cosh C_{34} h_1 C_{10} C_{34} C_{35} - \cosh C_{34} h_2 C_{10} C_{34} C_{35} - \right. \\ & \left. \sin \sqrt{C_{24}} h_1 \sqrt{C_{24}} C_{25} C_{36} + \sin \sqrt{C_{24}} h_2 \sqrt{C_{24}} C_{25} C_{36} - \right. \\ & \left. \cos \sqrt{C_{24}} h_1 \sqrt{C_{24}} C_{26} C_{36} + \cos \sqrt{C_{24}} h_2 \sqrt{C_{24}} C_{26} C_{36} \right) \\ & \left(-\cosh C_{34} h_1 C_{35} + \cosh C_{34} h_2 C_{35} - \sinh C_{34} h_1 C_{35} + \right. \\ & \left. \sinh C_{34} h_2 C_{35} - (\cosh C_{34} h_1 C_{34} C_{35} + \sinh C_{34} h_1 C_{34} C_{35})(-h_1 + h_2) \right) + \\ & \left(-\cosh C_{34} h_1 C_{34} C_{35} + \cosh C_{34} h_2 C_{34} C_{35} - \sinh C_{34} h_1 C_{34} C_{35} + \right. \\ & \left. \sinh C_{34} h_2 C_{34} C_{35} \right) \end{aligned} \right\}, \quad (3.38)$ $\left(\begin{aligned} & F + \sinh C_{34} h_1 C_{10} C_{35} - \sinh C_{34} h_2 C_{10} C_{35} + \cos \sqrt{C_{24}} h_1 C_{25} C_{36} - \\ & \cos \sqrt{C_{24}} h_2 C_{25} C_{36} - \sin \sqrt{C_{24}} h_1 C_{26} C_{36} + \sin \sqrt{C_{24}} h_2 C_{26} C_{36} - \\ & \left(1 - \cosh C_{34} h_1 C_{10} C_{34} C_{35} + \sin \sqrt{C_{24}} h_1 \sqrt{C_{24}} C_{25} C_{36} \right) (-h_1 + h_2) \\ & + \cos \sqrt{C_{24}} h_1 \sqrt{C_{24}} C_{26} C_{36} \end{aligned} \right)$	
$C_{40} = \left. \begin{aligned} & \left(-\cosh C_{34} h_1 C_{34} C_{35} + \cosh C_{34} h_2 C_{34} C_{35} - \right. \\ & \left. \sinh C_{34} h_1 C_{34} C_{35} + \right. \\ & \left. \sinh C_{34} h_2 C_{34} C_{35} \right) \\ & \left(-\cosh C_{34} h_1 C_{35} + \cosh C_{34} h_2 C_{35} - \right) \left(-\sinh C_{34} h_1 C_{34} C_{35} \right) \\ & \left(+\sinh C_{34} h_2 C_{34} C_{35} \right) \end{aligned} \right\}, \quad (3.39)$ $\left(\begin{aligned} & -\cosh C_{34} h_1 C_{35} + \cosh C_{34} h_2 C_{35} - \sinh C_{34} h_1 C_{35} + \\ & \sinh C_{34} h_2 C_{35} - \\ & (\cosh C_{34} h_1 C_{34} C_{35} + \sinh C_{34} h_1 C_{34} C_{35})(-h_1 + h_2) \end{aligned} \right)$	

$C_{41} = \left\{ \begin{array}{l} \left(\begin{array}{l} \cosh C_{34} h_1 C_{10} C_{34} C_{35} - \cosh C_{34} h_2 C_{10} C_{34} C_{35} - \\ \sin \sqrt{C_{24}} h_1 \sqrt{C_{24}} C_{25} C_{36} + \sin \sqrt{C_{24}} h_2 \sqrt{C_{24}} C_{25} C_{36} - \\ \cos \sqrt{C_{24}} h_1 \sqrt{C_{24}} C_{26} C_{36} + \cos \sqrt{C_{24}} h_2 \sqrt{C_{24}} C_{26} C_{36} \end{array} \right) \\ \left(\begin{array}{l} -\cosh C_{34} h_1 C_{35} + \cosh C_{34} h_2 C_{35} - \sinh C_{34} h_1 C_{35} + \\ \sinh C_{34} h_2 C_{35} - (\cosh C_{34} h_1 C_{34} C_{35} + \sinh C_{34} h_1 C_{34} C_{35}) \\ (-h_1 + h_2) \end{array} \right) \\ + \left(\begin{array}{l} -\cosh C_{34} h_1 C_{34} C_{35} + \cosh C_{34} h_2 C_{34} C_{35} - \sinh C_{34} h_1 C_{34} C_{35} + \\ \sinh C_{34} h_2 C_{34} C_{35} \end{array} \right) \\ \left(\begin{array}{l} F + \sinh C_{34} h_1 C_{10} C_{35} - \sinh C_{34} h_2 C_{10} C_{35} + \\ \cos \sqrt{C_{24}} h_1 C_{25} C_{36} - \cos \sqrt{C_{24}} h_2 C_{25} C_{36} - \sin \sqrt{C_{24}} h_1 C_{26} C_{36} \\ + \sin \sqrt{C_{24}} h_2 C_{26} C_{36} - \left(1 - \cosh C_{34} h_1 C_{10} C_{34} C_{35} + \sin \sqrt{C_{24}} h_1 \right) \\ \left(\sqrt{C_{24}} C_{25} C_{36} + \cos \sqrt{C_{24}} h_1 \sqrt{C_{24}} C_{26} C_{36} \right) \\ (-h_1 + h_2) \end{array} \right) \end{array} \right\}, \quad (3.40)$	
$C_{42} = \left\{ \begin{array}{l} \left(\cosh C_{34} h_1 - \cosh C_{34} h_2 + \sinh C_{34} h_1 - \sinh C_{34} h_2 \right) \\ \left(\begin{array}{l} -\cosh C_{34} h_1 C_{34} C_{35} + \cosh C_{34} h_2 C_{34} C_{35} - \sinh C_{34} h_1 C_{34} C_{35} \\ + \sinh C_{34} h_2 C_{34} C_{35} \end{array} \right) \\ \left(\begin{array}{l} -\cosh C_{34} h_1 C_{35} + \cosh C_{34} h_2 C_{35} - \\ \sinh C_{34} h_1 C_{34} C_{35} (-h_1 + h_2) \end{array} \right) - \left(\begin{array}{l} -\sinh C_{34} h_1 C_{34} C_{35} + \\ \sinh C_{34} h_2 C_{34} C_{35} \end{array} \right) \\ \left(\begin{array}{l} -\cosh C_{34} h_1 C_{35} + \cosh C_{34} h_2 C_{35} \\ -\sinh C_{34} h_1 C_{35} + \sinh C_{34} h_2 C_{35} - \left(\cosh C_{34} h_1 C_{34} C_{35} + \right) \\ \left(\sinh C_{34} h_1 C_{34} C_{35} \right) \\ (-h_1 + h_2) \end{array} \right) \end{array} \right\}, \quad (3.41)$	

$$C_{43} = \left. \begin{aligned} & \left(\cosh C_{34} h_1 C_{10} C_{34} C_{35} - \cosh C_{34} h_2 C_{10} C_{34} C_{35} - \sin \sqrt{C_{24}} h_1 \right. \\ & \left. \sqrt{C_{24}} C_{25} C_{36} + \sin \sqrt{C_{24}} h_2 \sqrt{C_{24}} C_{25} C_{36} - \cos \sqrt{C_{24}} h_1 \sqrt{C_{24}} C_{26} C_{36} \right. \\ & \left. + \cos \sqrt{C_{24}} h_2 \sqrt{C_{24}} C_{26} C_{36} \right) \\ & \left(-\cosh C_{34} h_1 C_{35} + \cosh C_{34} h_2 C_{35} \right. \\ & \left. -\sinh C_{34} h_1 C_{35} + \sinh C_{34} h_2 C_{35} - \left(\cosh C_{34} h_1 C_{34} C_{35} + \sinh C_{34} h_1 \right) \right. \\ & \left. \left(-h_1 + h_2 \right) \right) \left. \vphantom{\begin{aligned} & \left(\cosh C_{34} h_1 C_{10} C_{34} C_{35} - \cosh C_{34} h_2 C_{10} C_{34} C_{35} - \sin \sqrt{C_{24}} h_1 \right. \\ & \left. \sqrt{C_{24}} C_{25} C_{36} + \sin \sqrt{C_{24}} h_2 \sqrt{C_{24}} C_{25} C_{36} - \cos \sqrt{C_{24}} h_1 \sqrt{C_{24}} C_{26} C_{36} \right. \\ & \left. + \cos \sqrt{C_{24}} h_2 \sqrt{C_{24}} C_{26} C_{36} \right)} \right\}, \end{aligned} \quad (3.42)$$

$$+ \left(\begin{aligned} & -\cosh C_{34} h_1 C_{34} C_{35} + \cosh C_{34} h_2 C_{34} C_{35} \\ & -\sinh C_{34} h_1 C_{34} C_{35} + \sinh C_{34} h_2 C_{34} C_{35} \end{aligned} \right)$$

$$C_{44} = \left(\begin{aligned} & \left(\cosh C_{34} h_1 - \cosh C_{34} h_2 + \sinh C_{34} h_1 - \sinh C_{34} h_2 \right) \\ & \left(\begin{aligned} & -\cosh C_{34} h_1 C_{34} C_{35} + \\ & \cosh C_{34} h_2 C_{34} C_{35} - \\ & \sinh C_{34} h_1 C_{34} C_{35} + \\ & \sinh C_{34} h_2 C_{34} C_{35} \end{aligned} \right) \\ & \left(\begin{aligned} & -\cosh C_{34} h_1 C_{35} + \cosh C_{34} h_2 C_{35} - \\ & \sinh C_{34} h_1 C_{34} C_{35} (-h_1 + h_2) \end{aligned} \right) - \\ & \left(\begin{aligned} & -\sinh C_{34} h_1 C_{34} C_{35} \\ & + \sinh C_{34} h_2 C_{34} C_{35} \end{aligned} \right) \left(\begin{aligned} & -\cosh C_{34} h_1 C_{35} + \cosh C_{34} h_2 C_{35} - \\ & \sinh C_{34} h_1 C_{35} + \sinh C_{34} h_2 C_{35} - \\ & \left(\cosh C_{34} h_1 C_{34} C_{35} + \right) \\ & \left(\sinh C_{34} h_1 C_{34} C_{35} \right) (-h_1 + h_2) \end{aligned} \right) \end{aligned} \right) \quad (3.43)$$

$C_{45} = \frac{1}{2\sqrt{C_{24}C_{34}}(h_1 - h_2)}$	$\left. \begin{aligned} & 2C_{10}\sqrt{C_{24}}C_{35} \left(\begin{array}{c} -\cosh C_{34}h_2h_1 + \\ \cosh C_{34}h_1h_2 \end{array} \right) + \\ & 2C_{34}C_{36} \left(\begin{array}{c} C_{26} \left(\begin{array}{c} -\cos\sqrt{C_{24}}h_2h_1 \\ +\cos\sqrt{C_{24}}h_1h_2 \end{array} \right) \\ + C_{25} \left(\begin{array}{c} -\sin\sqrt{C_{24}}h_2h_1 \\ +\sin\sqrt{C_{24}}h_1h_2 \end{array} \right) \end{array} \right) \\ & + \sqrt{C_{24}} \left(\begin{array}{c} (E - C_{33})C_{34}h_1(h_1 - h_2)h_2 - \\ 2C_{31}C_{35}(-e^{C_{34}h_2}h_1 + e^{C_{34}h_1}h_2) + \\ 2C_{30}C_{35} \left(\begin{array}{c} \sinh C_{34}h_2h_1 - \\ \sinh C_{34}h_1h_2 \end{array} \right) \end{array} \right) \end{aligned} \right\} R_m,$	(3.44)
$C_{46} = -\frac{1}{2\sqrt{C_{24}C_{34}}(h_1 - h_2)}$	$\left. \begin{aligned} & 2 \left(\begin{array}{c} (\sin\sqrt{C_{24}}h_1 - \sin\sqrt{C_{24}}h_2)C_{25} + \\ (\cos\sqrt{C_{24}}h_1 - \cos\sqrt{C_{24}}h_2)C_{26} \end{array} \right) C_{34}C_{36} + \\ & \sqrt{C_{24}} \left(\begin{array}{c} \left(\begin{array}{c} \cosh C_{34}h_1 - \\ \cosh C_{34}h_2 \end{array} \right) \\ C_{10} + \left(\begin{array}{c} -\sinh C_{34}h_1 + \\ \sinh C_{34}h_2 \end{array} \right) C_{30} \\ - (e^{C_{34}h_1} - e^{C_{34}h_2})C_{31} \end{array} \right) C_{35} \\ & + (E - C_{33})C_{34}(h_1^2 - h_2^2) \end{aligned} \right\} R_m,$	(3.45)

3.3 Results and discussion

In this section, we discussed the effects of different physical parameters, nanoparticle volume fraction ϕ , Stommer's number S_1 , magnetic Reynolds R_m , heat generation Q_0 and shape factor m of the nanoparticles on pressure rise, Stommer's number S_1 , magnetic Reynolds R_m , Grashof number Gr and shape factor m on pressure gradient, nanoparticle volume fraction ϕ , heat generation Q_0 and shape factor m of the nanoparticles on the temperature, magnetic Reynolds R_m and Stommer's number S_1 as well as shape factor m of the nanoparticles on axial induced magnetic field h_x and current density j_z , nanoparticle volume fraction ϕ , Stommer's number S_1 , magnetic Reynolds R_m and Grashof number Gr and generation Q_0 on the velocity profiles for copper nanofluid of shape bricks cylinder and platelets with the help of graphical results displayed in Figs. (3.1) – (3.4). The trapping bolus phenomenon observing the flow behavior is also manipulated as well with the help of streamlines graphs in the Figs. (3.7) – (3.12).

From Figs. 3.1(a) – 3.1(c) one can see that pressure rise increases with the increase of volume fraction ϕ , Stommer's number S_1 and magnetic Reynolds R_m . Fig.3.1 (d) shows that Δp decreases with the increase of Q_0 .

If all other parameters are kept constant and give variation to shape factor m then pressure rise is an increasing function of m .

Fig. 3.2 (a) Represents the effects of volume fraction on the pressure gradient dp/dx . It is measured that as one can increase the value of volume fraction pressure gradient decreases. Figs. 3.2 (b) and 3.2 (c) shows that dp/dx increases with the increase of Stommer's number S_1 and magnetic Reynolds R_m . Fig. 3.2(d) shows that pressure gradient dp/dx is decreasing function of Gr . If all other parameters are kept constant and give variation to shape factor m then pressure rise is an increasing function except of volume fraction, for volume fraction dp/dx is decreasing function of m .

Fig. 3.3(a) shows the effects of temperature θ for the different values of volume fraction ϕ one can see that temperature decreases with increase of volume fraction ϕ , but increases with the increases of heat generation parameter Q_0 . If all other

parameter is kept constant and gives the variation to shape factor m then pressure rise is a decreasing function of m .

Fig. 3.4(a) shows the effect of magnetic Reynolds R_m on an axial induced magnetic field h_x against y . Axial induced magnetic field h_x increases in the half region of the channel but decreases in the remaining half region of the channel as one can increase the value of magnetic Reynolds R_m . Fig. 3.4(b) shows that Stommer's number gives the same behavior on an Axial induced magnetic field, If one increases the value of Stommer's number S_1 the value of h_x increases from wall h_1 to the middle of channel

Figs. 3.5(a) and 3.5(b) show the variation of magnetic Reynolds and Stommer's number on current density j_z versus y . Fig. 3.5(a) shows that j_z is the increasing function of magnetic Reynolds and 3.5(b) shows that j_z is the decreasing function of Stommer's number when other parameters are kept constant.

Fig. 3.6(a) represents the effect of volume fraction on the velocity profile u . Velocity profile near to both sides of the channel decreases with the increase of volume fraction, but increases in the center of the channel. Fig. 3.6(b) and Fig. 3.6(c) represents the effect of Stommer's number and magnetic Reynolds on the velocity profile u . Velocity profile near to both sides of the channel increases with the increase of Stommer's number and magnetic Reynolds, but decrease in the center of the channel. Fig. 3.6(d) and Fig. 3.6(e) show opposite behavior of Grashof number and heat generation on the velocity profile u compare with the effect of Stommer's number and Grashof number. Velocity profile near to both sides of the channel decreases with the increase of volume fraction, but increase in the center of the channel. One can see that velocity profile u is a decreasing function of m near to both the wall of the channel but increasing function of m at the center of the channel.

A very interesting phenomenon in the fluid transport is trapping. In the wave frame, streamlines under certain circumstances swell to trap a bolus which travels as an inlet with the wave speed. The occurring of an internally circulating bolus stiffened by closed streamline is called trapping. The bolus described as a volume of fluid bounded by a closed streamlines in the wave frame is moved at the wave pattern. Fig. 3.7 indicates the streamlines for the various values of the parameter ϕ . It is observed that for greater values of ϕ the size of bolus becomes larger in case of bricks shape nanoparticles. Same behavior is seen in Fig. (3.8) and (3.9) for cylinder and platelet

shape nanoparticles respectively. Fig. (3.10) is drawn for the nano copper fluid with particle shape bricks, it is noticed that greater values of Gr bolus becomes small. Same behavior is seen in Figs. (3.11) and (3.12) for cylinder and platelet shape nanoparticles respectively.

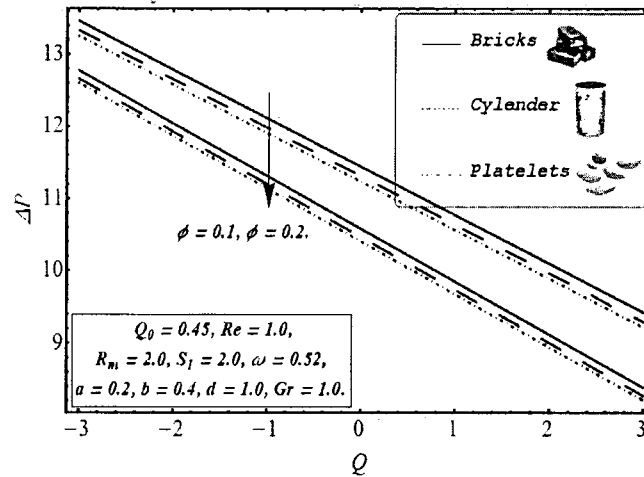


Fig. 3.1 (a): Variation of pressure rise Δp for different value of ϕ .

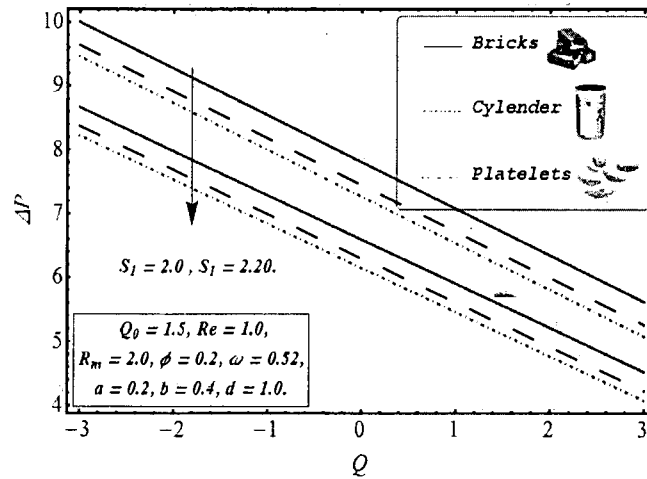


Fig. 3.1 (b): Variation of pressure rise Δp different value of S_1 .

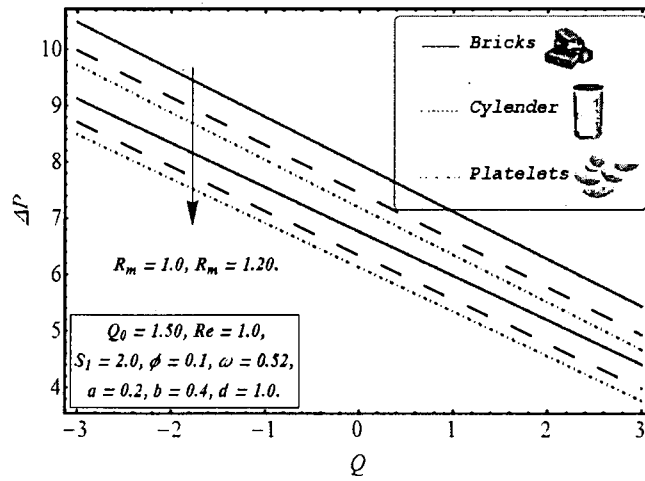


Fig. 3.1 (c): Variation of pressure rise Δp different value of R_m .

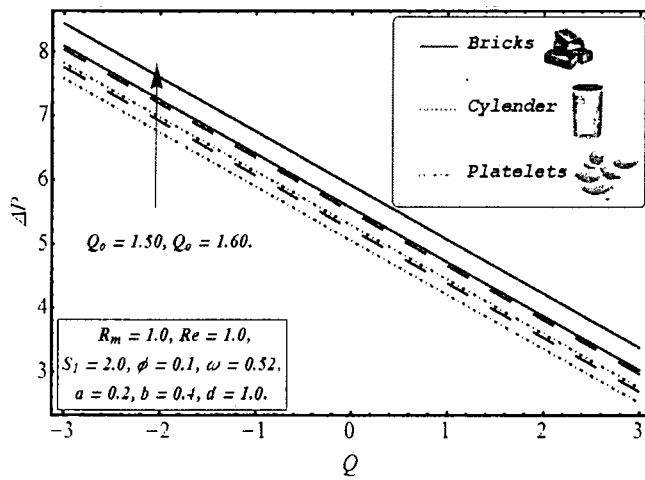


Fig. 3.1 (a): Variation of pressure rise Δp different value of Q_0 .

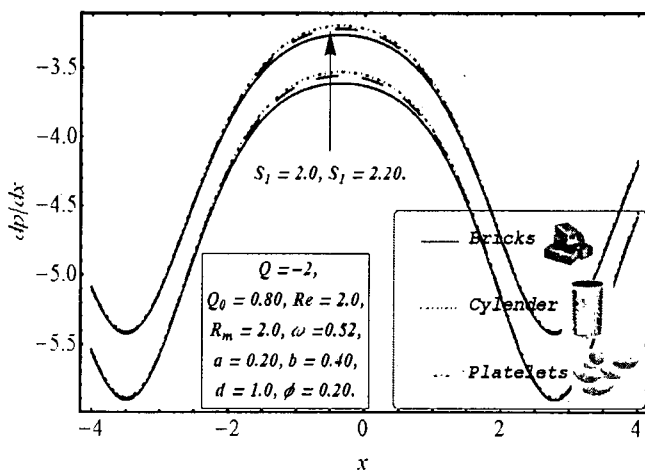


Fig. 3.2 (b): Variation of pressure gradient dp/dx different value of S_1 .

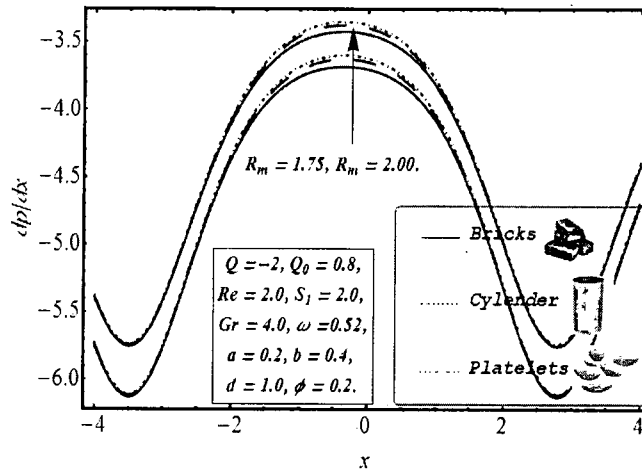


Fig. 3.2 (c): Variation of pressure gradient dp/dx different value of R_m .

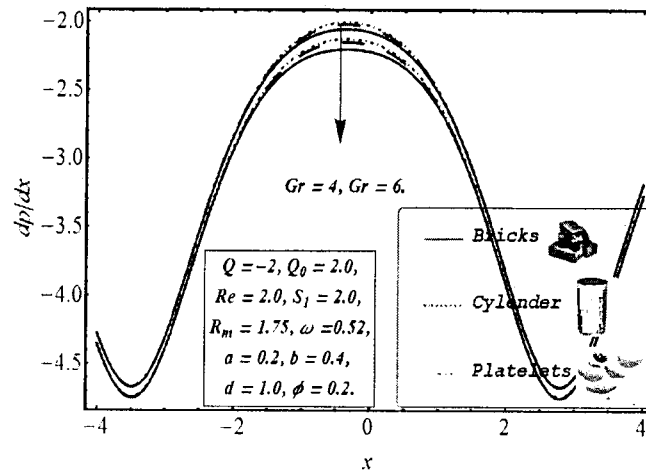


Fig. 3.2 (d): Variation of pressure gradient dp/dx different value of Gr .

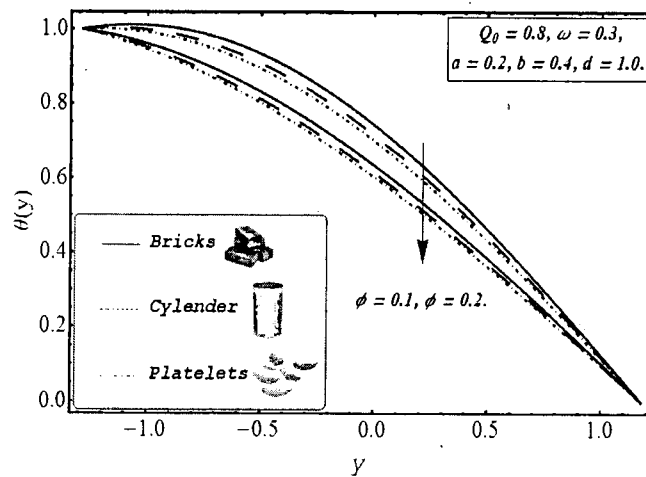


Fig. 3.3 (a): Variation of temperature profile θ different value of ϕ .

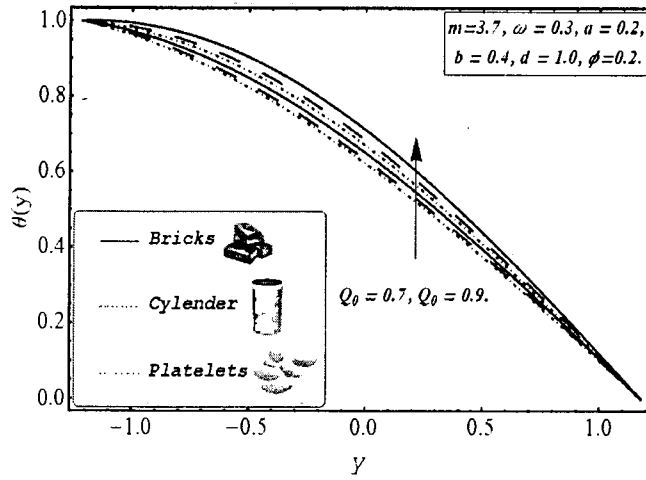


Fig. 3.3 (b) : Variation of temperature profile θ different value of Q_0 .

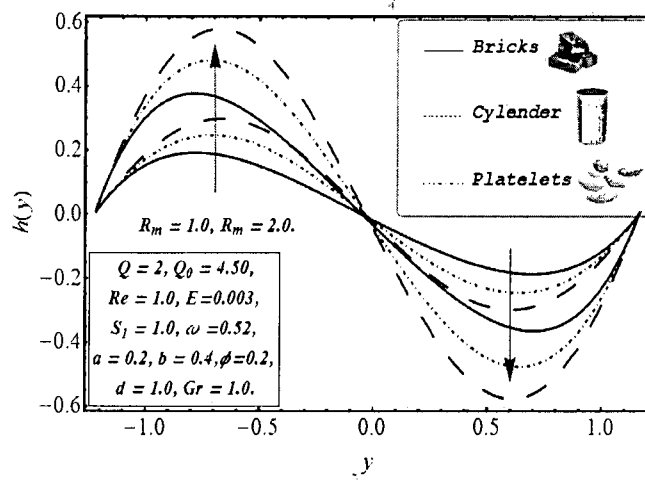


Fig. 3.4 (a): Variation of axial induced magnetic field h_x for different value of R_m .

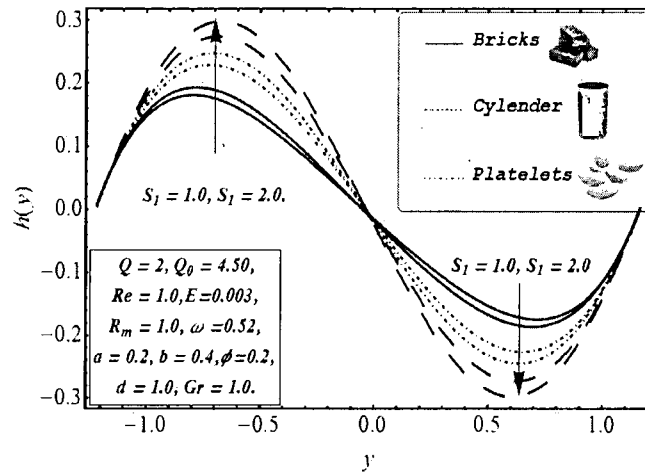


Fig. 3.4 (b): Variation of axial induced magnetic field h_x for different value of S_1 .

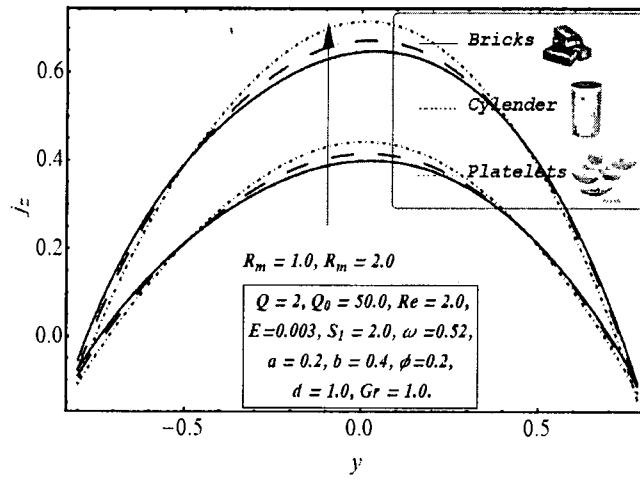


Fig. 3.5 (a): Variation of current density j_z for different values of R_m .

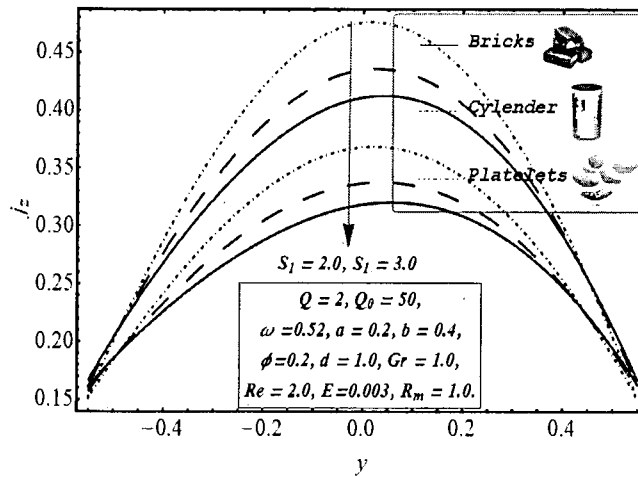


Fig. 3.5 (b): Variation of current density j_z for different values of S_1 .

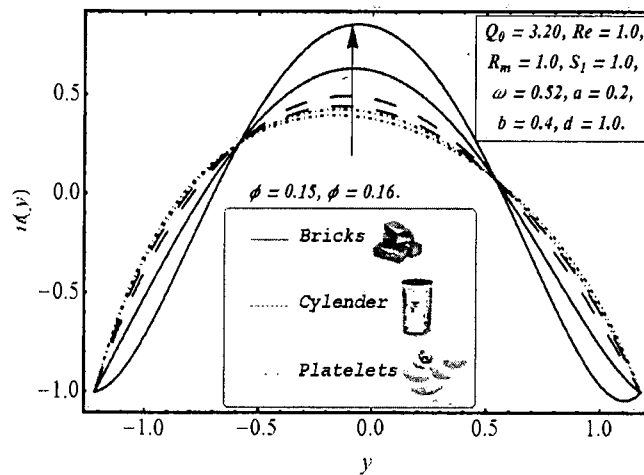


Fig. 3.6 (a): Variation of velocity profile $u(y)$ different value of ϕ .

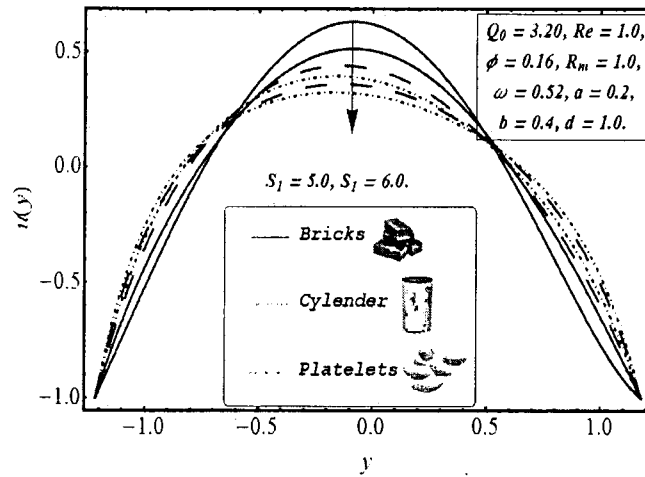


Fig. 3.6 (b): Variation of velocity profile $u(y)$ for different values of S_1 .

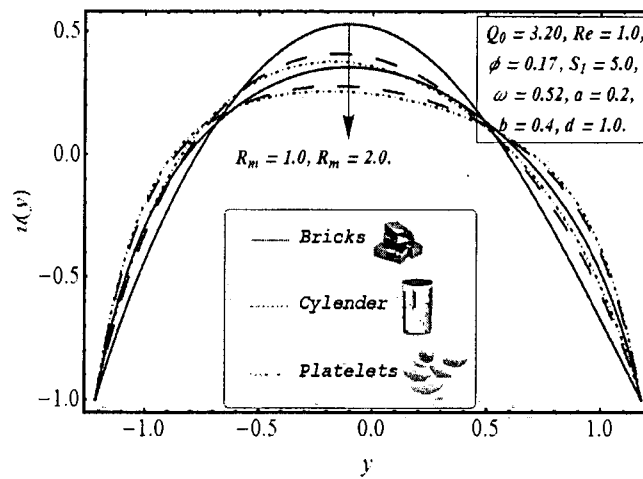


Fig. 3.6 (c): Variation of velocity profile $u(y)$ for different values of R_m .

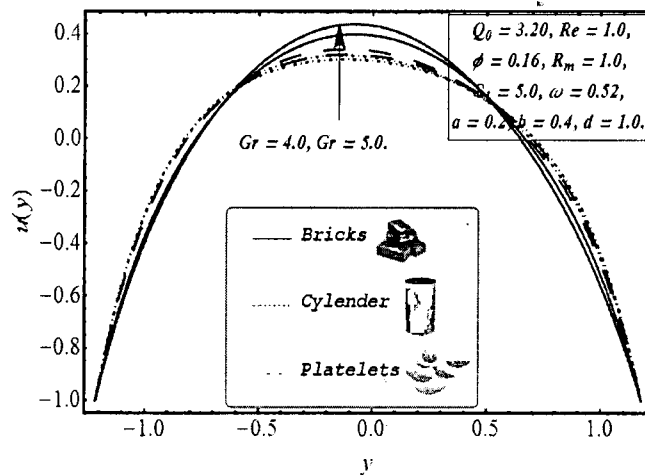


Fig. 3.6 (d): Variation of velocity profile $u(y)$ for different values of Gr .

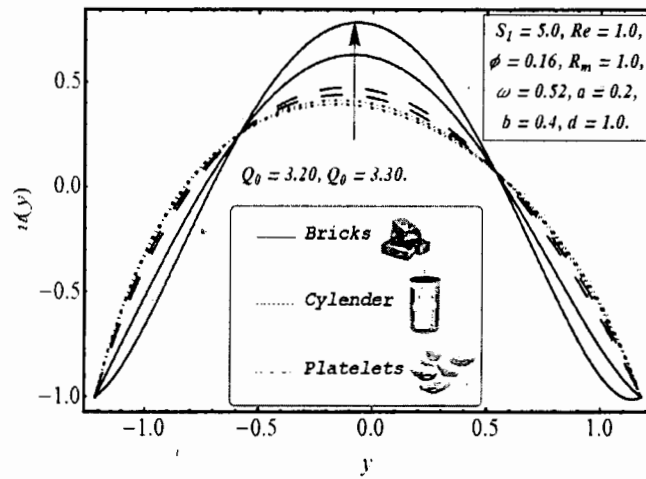
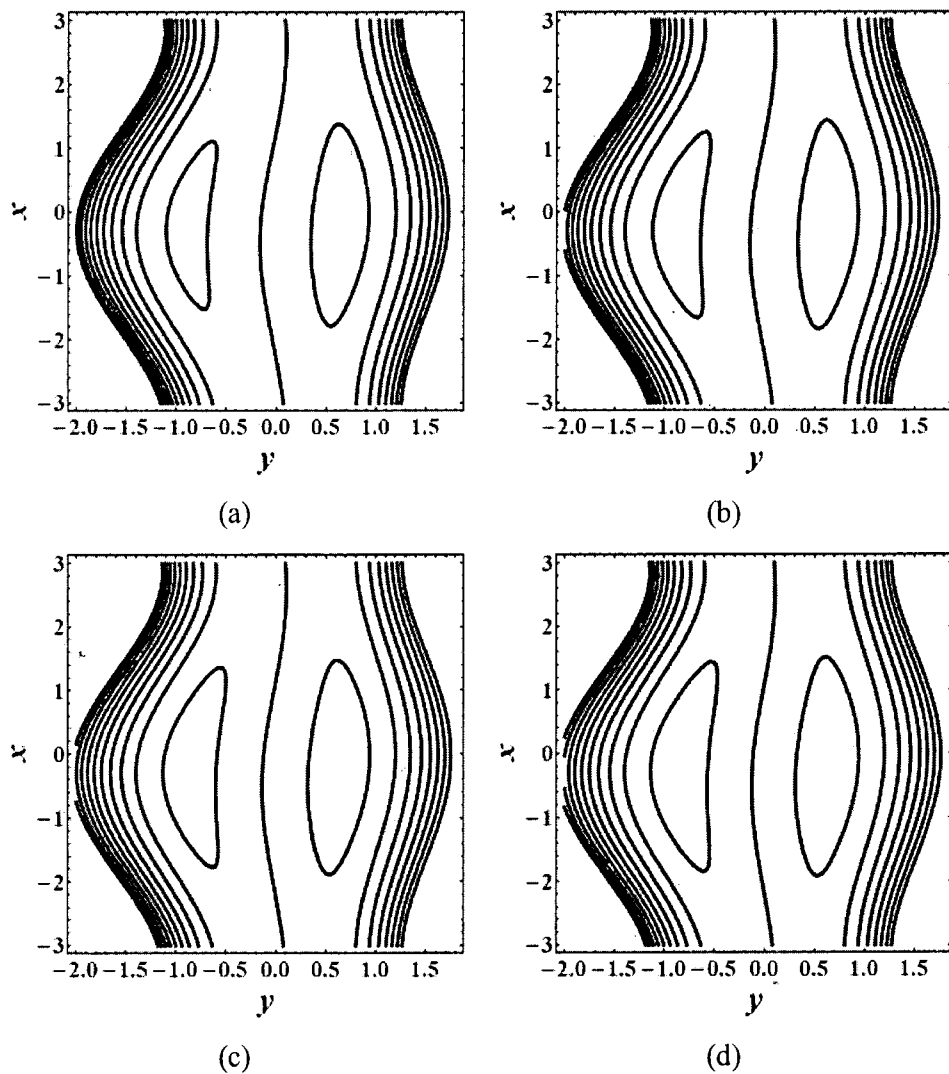
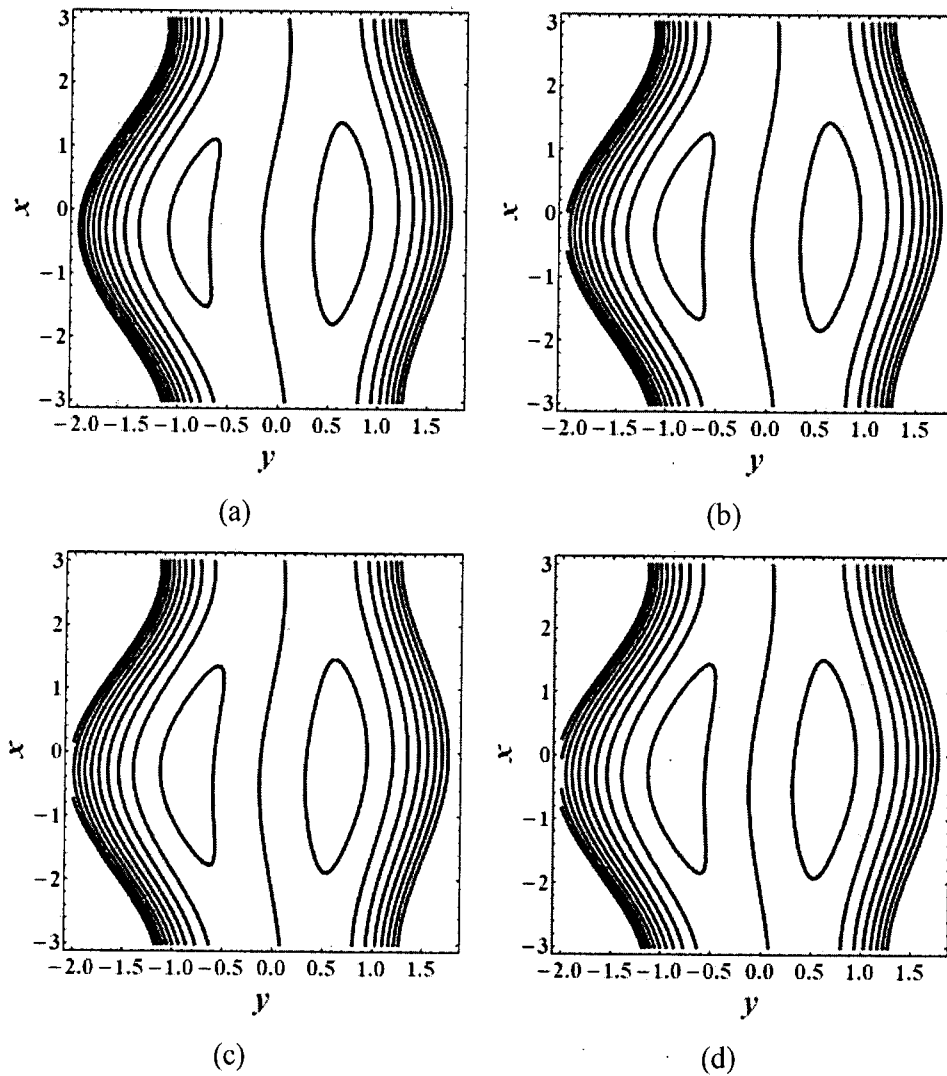


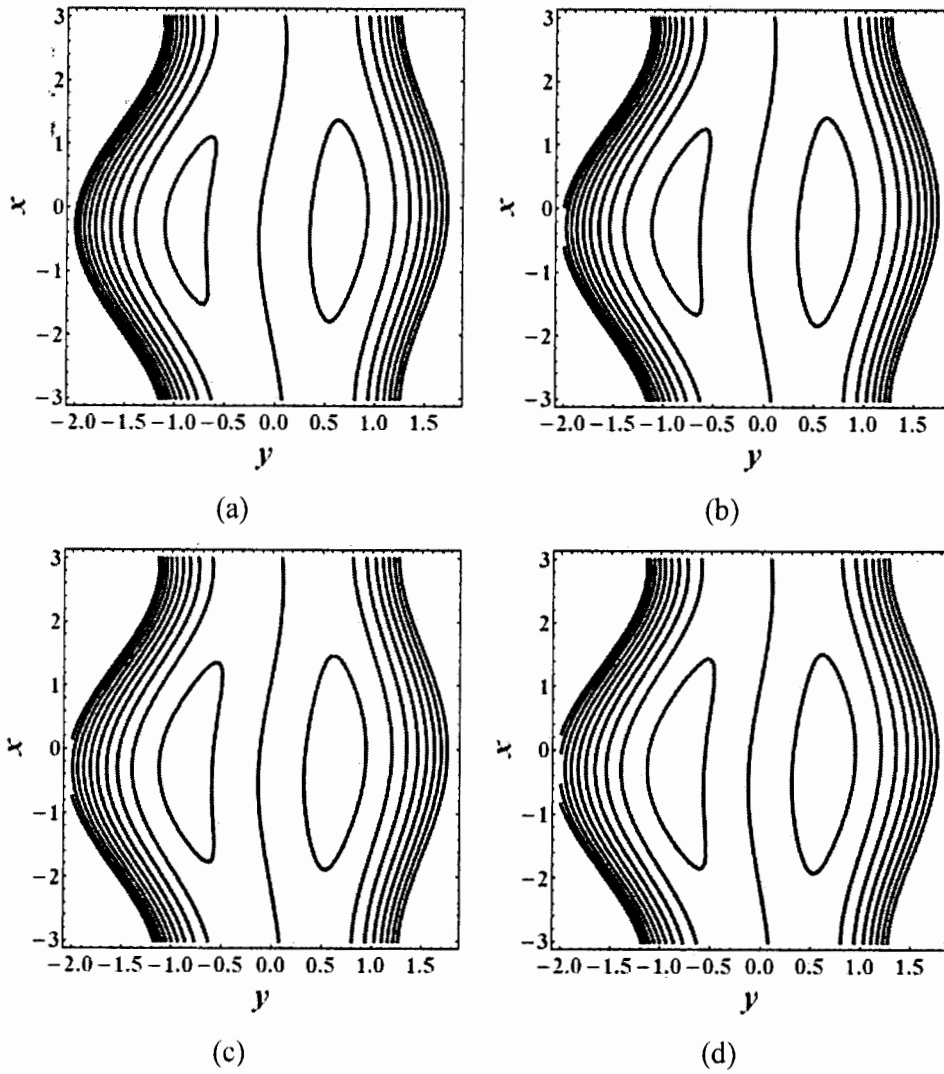
Fig.3.6 (e): Variation of velocity profile $u(y)$ for different values of Q_0 .



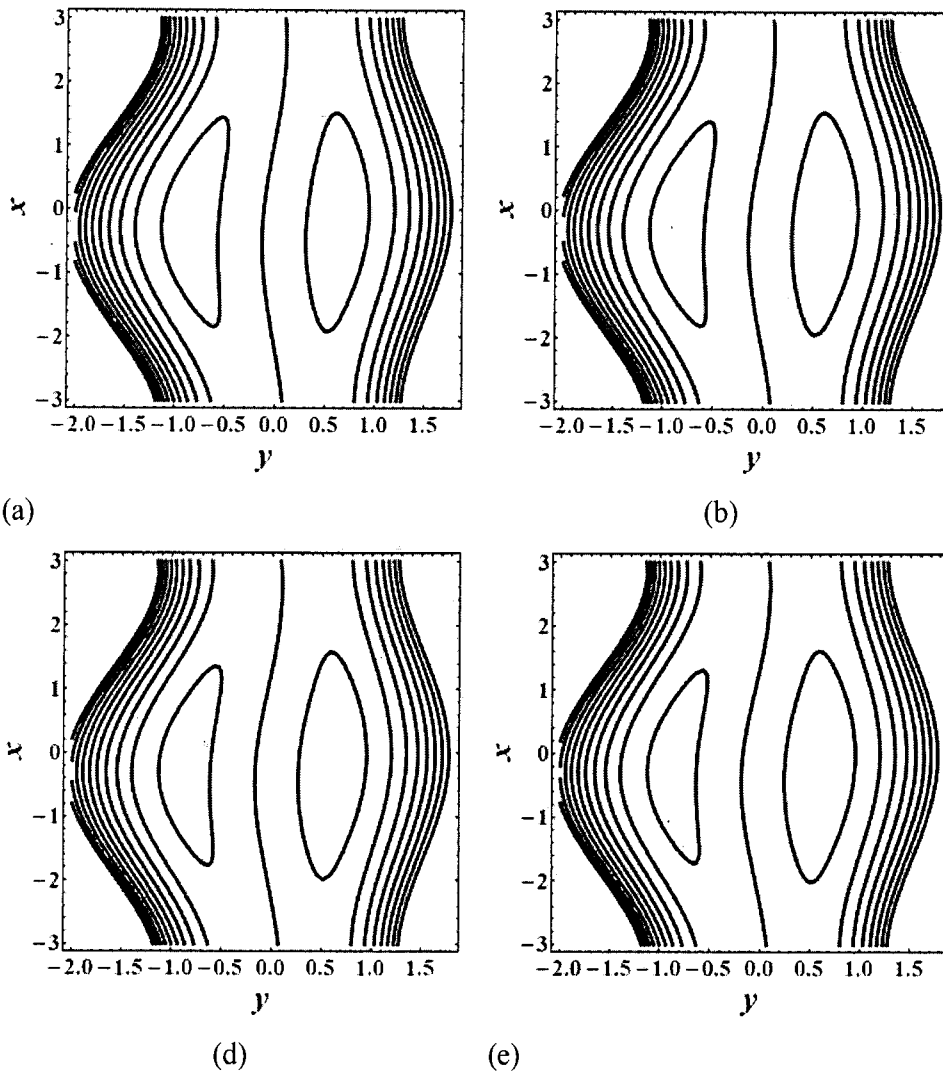
Figs.3. 7: Stream lines of bricks shape nanoparticles for different values of ϕ . (a) for $\phi = 0.1$, (b) for $\phi = 0.2$, (c) for $\phi = 0.3$, (d) for $\phi = 0.4$. The other parameters are $Q = 2$, $\omega = 0.3$, $a = 0.2$, $b = 0.4$, $d = 1.0$, $Gr = 1$, $R_m = 1.0$, $S_1 = 2$, $Re = 1.0$, $Q_0 = 0.1$.



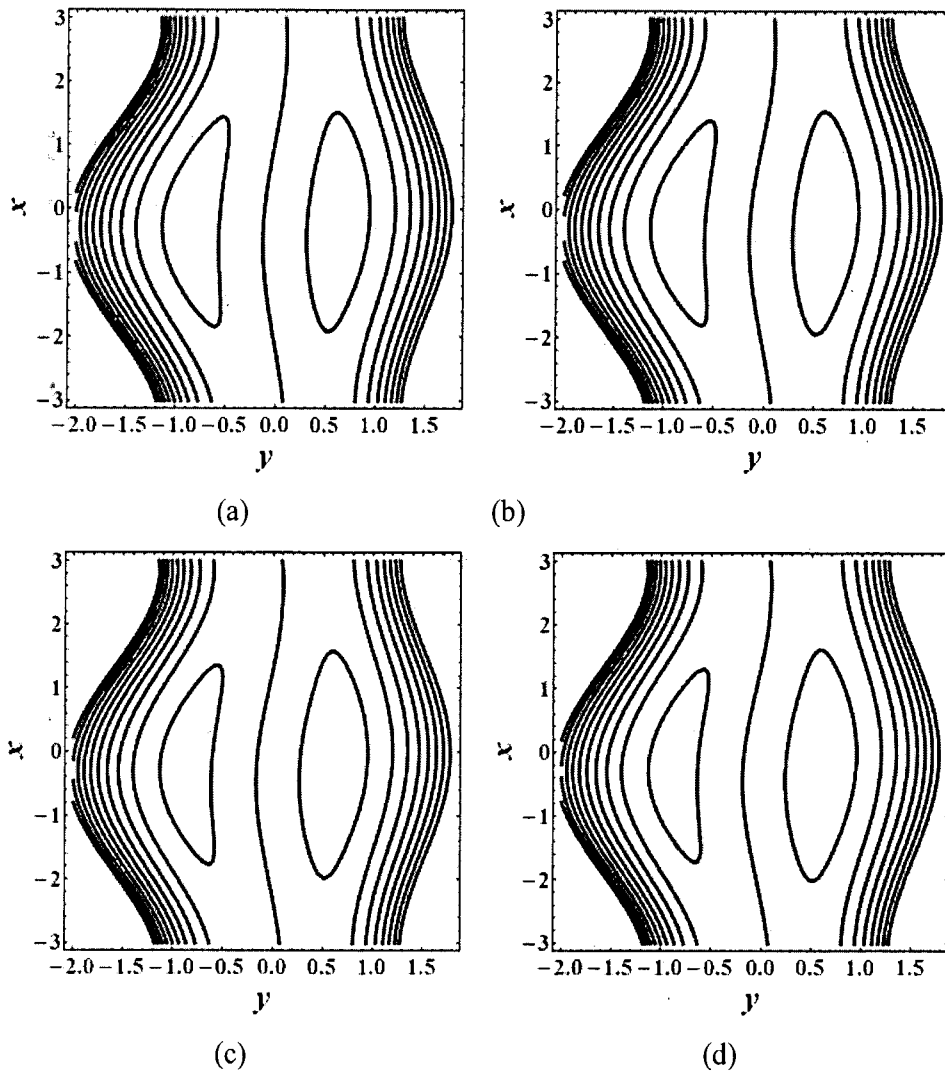
Figs.3. 8: Stream lines of cylinder shape nanoparticles for different values of ϕ . (a) for $\phi = 0.1$, (b) for $\phi = 0.2$, (c) for $\phi = 0.3$, (d) for $\phi = 0.4$. The other parameters are $Q = 2$, $\omega = 0.3$, $a = 0.2$, $b = 0.4$, $d = 1.0$, $Gr = 1$, $R_m = 1.0$, $S_1 = 2$, $Re = 1.0$, $Q_0 = 0.1$.



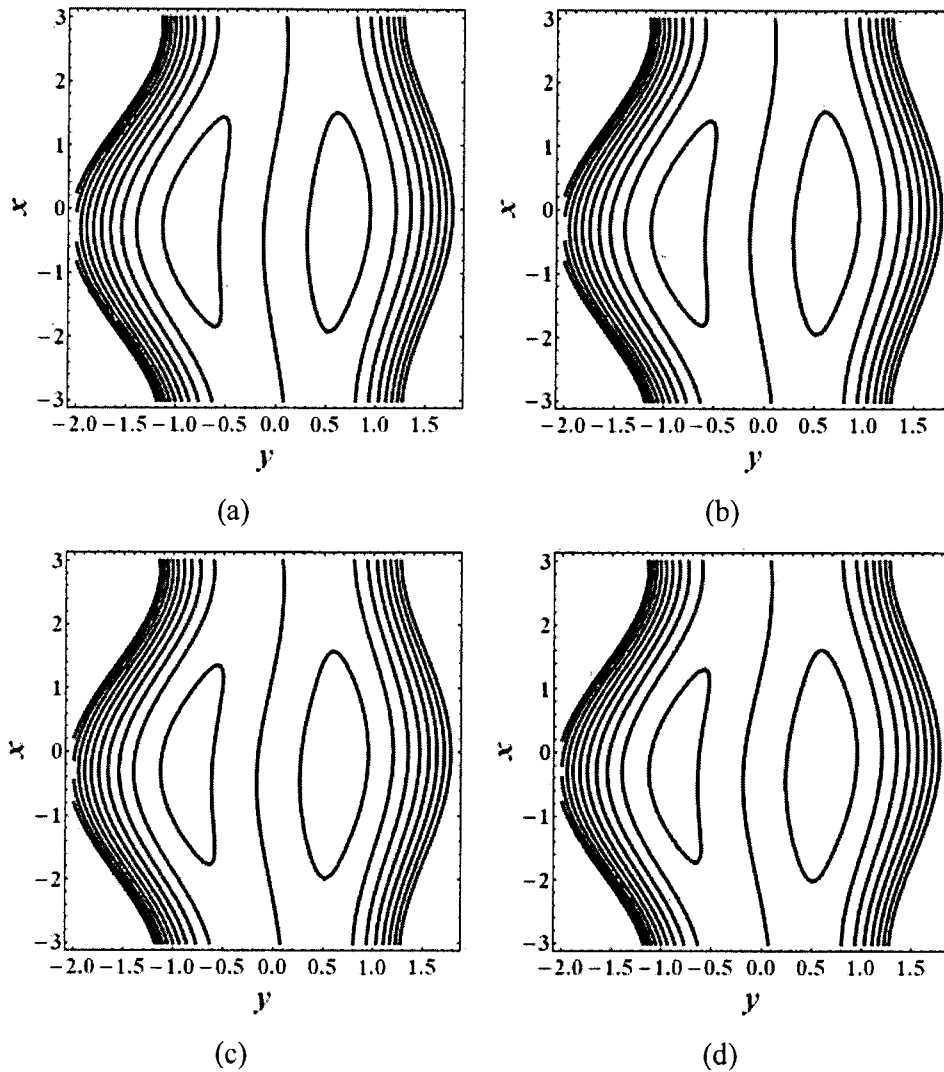
Figs. 3.9: Stream lines of platelets shape nanoparticles for different values of ϕ . (a) for $\phi = 0.1$, (b) for $\phi = 0.2$, (c) for $\phi = 0.3$, (d) for $\phi = 0.4$. The other parameters are $Q = 2$, $\omega = 0.3$, $a = 0.2$, $b = 0.4$, $d = 1.0$, $Gr = 1$, $R_m = 1.0$, $S_1 = 2$, $Re = 1.0$, $Q_0 = 0.1$.



Figs. 3.10: Stream lines of bricks shape nanoparticles for different values of Gr . (a) for $Gr=1$, (b) for $Gr=2$, (c) for $Gr=3$, (d) for $Gr=4$. The other parameters are $Q=2$, $\omega=0.3$, $a=0.2$, $b=0.4$, $d=1.0$, $\phi=0.4$, $R_m=1.0$, $S_1=2$, $Re=1.0$, $Q_0=0.1$.



Figs. 3.11: Stream lines of cylinder shape nanoparticles for different values of Gr . (a) For $Gr=1$, (b) for $Gr=2$, (c) for $Gr=3$, (d) for $Gr=4$. The other parameters are $Q=2$, $\omega=0.3$, $a=0.2$, $b=0.4$, $d=1.0$, $\phi=0.4$, $R_m=1.0$, $S_1=2$, $Re=1.0$, $Q_0=0.1$.



Figs. 3.12: Stream lines of platelets shape nanoparticles for different values of Gr . (a) For $Gr=1$, (b) for $Gr=2$, (c) for $Gr=3$, (d) for $Gr=4$. The other parameters are $Q=2, \omega=0.3, a=0.2, b=0.4, d=1.0, \phi=0.4, R_m=1.0, S_1=2, Re=1.0, Q_0=0.1$.

3.4 Conclusion

Interaction of nanoparticles for the peristaltic flow with the induced magnetic field is discussed, key points are observed as follows:

- i. It is measure that pressure rise is an increasing function of volume fraction, Stommer's number and magnetic Reynolds number as well as shape factor .
- ii. Pressure rise is a decreasing function of heat generation.

- iii. It is observed that pressure gradient gets increased as one can increase the value of Stommer's number and magnetic Reynolds number, but decreased with the increasing effect of Grashof number and volume fraction.
- iv. For different values of shape factor m one can see that pressure gradient is an increasing function of m .
- v. It is noticed that temperature gets decrease with the increase of volume fraction but increases as one can increases the value of heat generation.
- vi. Temperature is a decreasing function of shape factor m .
- vii. The value of velocity decreases near to both side of the channel but increases at the center of the channel as one can increase the value of volume fraction, Grashof number and heat generation.
- viii. It is observed that velocity gets increase near to both side of channel with the increase of Stommer's number and magnetic Reynolds number but have opposite behavior at the center the of the channel. At the center of the channel velocity decreases with the increase of Stommer's number and magnetic Reynolds number.
- ix. One can see in the figure that near to side of channel velocity is increasing function of shape factor and decreasing at the center of the channel.
- x. It is measured that for greater value of volume fraction bolus becomes large.
- xi. For greater value of Grashof number bolus becomes smaller.

References

- [1]. Choi S.U.S, Enhancing thermal conductivity of fluids with nanoparticles, proceeding of ASME International Mechanical Engineering Congress and Exposition, San Francisco, (1995) 99 – 105.
- [2]. Buongiorno J, Convective transport in nanofluids, *Journal Heat Transfer*, 128 (2006) 240 – 250.
- [3]. Xuan Y, Roetzel W, Conceptions for heat transfer correlation of nanofluids, *International Journal Heat Mass Transfer*, 43 (2000) 3701 – 3707.
- [4]. Khanafer K, Vafai K, Lightstone M, Buoyancy-driven heat transfer enhancement in a two-dimensional enclosure utilizing nanofluids, *International Journal Heat Mass Transfer*, 46 (2003) 3639 – 3653.
- [5]. Das S. K, Putra N, Roetzel W, Pool boiling characteristics of nanofluids, *International Journal Heat Mass Transfer*, 46 (2003) 851 – 862.
- [6]. Xie H, Lee H, Youn W, Choi M. Nanofluids containing multiwalled carbon nanotubes and their enhanced thermal conductivities. *Journal of Applied Physics*, 94 (2003) 4967 – 4971.
- [7]. Kuznetsov A. V, Nield D. A, Natural convective boundary layer flow of a nanofluid past a vertical plate, *International Journal of Thermal Science*, 49 (2010) 243 – 247.
- [8]. Makinde O. D, Aziz A, Boundary layer flow of a nanofluid past a stretching sheet with a convective boundary condition, *International Journal of Thermal Science*, 50 (2011) 1326 – 1332.
- [9]. Aziz A, Khan W. A, Natural convective boundary layer flow of a nanofluid past a convectively heated vertical plate, *International Journal of Thermal Science*, 52 (2012) 83 – 90.
- [10]. Emad H. A, Ebaid A, Exact analytical solution for suction and injection flow with thermal enhancement of five nanofluids over an isothermal stretching sheet with effect of the slip model: A comparative study, *Abstract and Applied Analysis*, (2013), Article ID 721578, 2013.
- [11]. Latham T. W, Fluid motion in a peristaltic pump, MS. Thesis, Massachusetts Institute of Technology, Cambridge, (1966).

- [12]. Shapiro A. H, Jaffrin M. Y, Weinberg S. L, Peristaltic pumping with long wavelengths at low Reynolds number, *Journal of Fluid Mechanics*, 37 (1969) 799 – 825.
- [13]. Noreen S. A, Nadeem S, Endoscopic effects on the peristaltic flow of a Jeffrey six-constant fluid model with variable viscosity, *Journal of Aerospace Engineering*, 26 (2013) 535 – 543.
- [14]. Srinivas S, Gayathri R, Kothandapani M, The influence of slip conditions, 13 wall properties and heat transfer on Magnetohydrodynamic peristaltic transport, *Computer Physics Communications*, 180 (2009) 2115 – 2122.
- [15]. Noreen S. A, Nadeem S, Mixed convective Magnetohydrodynamic peristaltic flow of a Jeffrey nanofluid with Newtonian heating, *Zeitschrift für Naturforschung A*, 68 (2013) 433 – 441.
- [16]. Noreen S. A, Eyring Prandtl fluid flow with convective boundary conditions in small intestines, *International Journal of Biomathematics*, 6 (2013) 350034.
- [17]. Oztop H. F, Abu – Nada E, Numerical study of natural convection in partially heated rectangular enclosures filled with nanofluids, *International Journal of Heat and Mass Transfer*, 29 (2008) 1326 – 1336.
- [18]. Noreen S. A, Mohsin R, Ellahi R, Interaction of nano particles for the peristaltic flow in an asymmetric channel with the induced magnetic field, *The European Physical Journal Plus*, 129 (2014).
- [19]. Pastoriza M. J, Lugo L, Legido J. L, Piriciro M.M, Thermal conductivity and viscosity measurements of ethylene glycol – based Al_2O_3 nanofluids, *Nanoscale Research Letters*, 6 1/221, 2011.
- [20]. Jamshidi N, Farhadi M, Ganji D. D, Sedighi K, Experimental investigation on the viscosity of nanofluids, *International Journal of Engineering*, 25 (2012), 201 – 209.
- [21]. Timofeeva E. V, Routbort J. L, Singh D, Particle shape effects on thermophysical properties of alumina nanofluids, *Journal of Applied Physics*, 106 (2009) 014304.